UNITED STATES DISTRICT COURT
FOR THE DISTRICT OF DELAWARE

THE UNIVERSITY OF CHICAGO and BIO-RAD LABORATORIES, INC.	)	
Plaintiffs,	)	
v.	)	**C.A. 15-152-RGA**
10X GENOMICS, INC.	)	
Defendant.	)	

THE BROAD INSTITUTE, INC.'S LETTER MEMORANDUM
AS *AMICUS CURIAE* NOT IN SUPPORT OF ANY PARTY

The Broad Institute, Inc. ("Broad") is a unique non-profit research organization with its principal laboratories and offices located in Cambridge, Massachusetts and provides the following as its *amicus curiae* Letter Memorandum in the above-captioned litigation ("the subject litigation") not in support of any party. Familiarity with Broad's Motion for Leave to Participate as *Amicus Curiae* Not in Support of Any Party (cited herein as "Broad *Amicus Curiae* Motion") is presumed, with care taken to avoid repeating information as to Broad provided therein.

As discussed in the Broad *Amicus Curiae* Motion, Broad extensively uses single-cell genomics technology at issue, including with many ongoing techniques, programs, centers and participation in US Government and International programs, including the Broad Epigenomics Program, the Broad Cell Circuits Program, the Broad Center for Cell Circuits, the Broad Genetic Perturbation Platform and Functional Genomics Consortium, the Broad Cancer Program, the Klarman Cell Observatory, the Broad Program in Medical and Population Genetics, Drop Seq, Perturb Seq, RNA-Seq, sNuc-Seq, DroNc-Seq, the Cancer Moonshot and the Human Cell Atlas.

I. Background

It is understood that issues before the Court include whether there should be a permanent injunction against 10X, if there is such an injunction, the scope, content and timing of the injunction, as well as whether 10X products should incur a 15% ongoing royalty rate.

It is understood that the law sets forth factors that the Court is to analyze in determining whether to enter a permanent injunction after a finding that valid patent claims have been infringed. These factors include whether public interest would be served or disserved by a permanent injunction. It is also understood that the decision to grant or deny a permanent injunction as to 10X products, and the scope, content and timing of any such injunction, or to issue judgment imposing an ongoing royalty on 10X products is an act of equitable discretion of the Court.

Imposing a permanent injunction against 10X, especially if such injunction were to be immediate and of such a scope that 10X will be unable to continue to support existing customers of its equipment, would do a great disservice to the public interest. An immediate and broad injunction will significantly set back the research of Broad and other academic and/or not-for-profit research organizations. Such an injunction would call for, amongst other things, re-doing work already done to ensure that the results are compatible across different machines and tools and protocols or for further efforts to benchmark and compare results, at costs that are not able to be recovered by academic and/or not-for-profit research organizations. In addition, an immediate and broad injunction would require time to get new machines in place and running and will mean the loss of incoming biological samples (especially from humans) as such could not be done in sufficient time to allow research to continue seamlessly. Indeed, just the loss of experience with the existing tools and the needed retraining on new machines would place a great burden on academic institutions doing research using 10X machines.

II. Public Interest Weighs in Not Entering an Injunction

The public interest weighs in not entering a permanent injunction in situations such as this (here on 10X products), especially as to academic and/or not-for-profit research organizations, such as Broad, MIT, Harvard, Harvard-affiliated hospitals, and Broad's collaborators around the world, and especially with regard to current ongoing single-cell genomics research. At a minimum, the scope and timing of any injunction must be tailored to address the public interest in this regard.

The clear accommodation to the public interest is especially appropriate here as it is understood that the technology of the patents-in-suit was developed, at least in part, through the use of US public funds—US Government grant money. Thus, especially on this basis, the technology determined to be an infringement should not be permanently enjoined particularly with respect to academic and/or not-for-profit research organizations, and especially those that have already invested significant time and funds in research that includes the use of 10X instruments, reagents and protocols in ongoing research projects that will be irreparably damaged by such remedies.

Given that ongoing and future single-cell genomics research, as is the case with much research, generally requires continuity of laboratory instruments, reagents and protocols so that results can be considered comparable, and given that the instruments of 10X that are already in use are not fungible or able to be substituted by alternative instruments from Bio-Rad or others, on this basis too, the 10X technology accused of infringement should not be permanently enjoined or subject to an onerous royalty rate with respect to academic and/or not-for-profit research organizations in the continued use of such technology. Any lacuna in the ability to use such instruments will also cause existing and incoming samples to be wasted as labs attempt to

replace equipment and get back up to speed with new equipment so that research can begin again.

Broad thus suggests that, at least as to academic and/or not-for-profit organizations, such as Broad, MIT, Harvard, Harvard-affiliated hospitals, and Broad's collaborators around the world, the Court in assessing a proper remedy should use its equitable powers to allow 10X's products to continue to be available, and available at a reasonable price (i.e., no unreasonably high royalty is required for research use), as that is what is in the public interest.

Should the Court nonetheless determine, after an appropriate weighing of all of the relevant facts and factors, that an injunction is an appropriate long-term remedy with regard to the adjudged infringing products, given the burden of changeover, Broad requests that implementation of the injunction take place over at least a 9 month phase-in period, during which reagents are available for use with previously purchased 10X instruments, and that such phase-in period commence only after this action, and all appeals thereof, is complete.

Further, in view of ongoing work plans and plans as part of US Government projects with set budgets, Broad suggests that it would be in the public interest if new 10X instruments and reagents continue to be available to allow completion of established work plans and research in process. Alternatively, at a minimum, Broad requests that 10X reagents continue to be available for academic and non-profit research use with previously purchased instruments.

A. Technology in Litigation was Developed Through Use of Public Monies

Research that is supported by US Government funding (public monies) should not be the basis of patents for research tools where the patents are then used to restrict the ability for the public and for research institutions to use those research tools—especially as to further projects that are US Government projects—the US Government funding dictates that the tools developed be made available for use in research by the public. (Broad expresses no view on whether

commercial for-profit entities should be treated differently, especially where the technology is used directly to support their profitability.)

That subject litigation technology, e.g., subject matter of US Patent No. 8,889,083 ("the '083 patent") was developed through the use of US public monies—US Government funding—mandates that the technology, including as may be embodied in 10X's products, be kept freely and fairly available to academic and/or not-for-profit organizations, such as Broad, MIT, Harvard, Harvard-affiliated hospitals, and Broad's collaborators around the world.

Often, the patents themselves recite the use of US Government funding—here that is not the case, but to demonstrate that US Government funding was instrumental to work that developed the technology of patents-in-suit, (a fact that Plaintiffs should acknowledge), submitted herewith as Exhibit H is a copy of Song et al., "A Microfluidic System for Controlling Reaction Networks in Time" Angewandte Chemie International Edition 42:768-772 (17 Feb 2003), doi.org/10.1002/anie.200390203 ("Song") and as Exhibit I Tice et al., "Formation of Droplets and Mixing in Multiphase Microfluidics at Low Values of the Reynolds and the Capillary Numbers," Langmuir 19(22): 9127–9133 (12 Aug 2003), DOI: 10.1021/la030090w ("Tice").

Both Song and Tice state, "This work was supported by . . . Chicago MRSEC funded by the NSF." The "MRSEC" is the Materials Research Science and Engineering Center (MRSEC) at the University of Chicago (*see* https://mrsec.uchicago.edu/about). The "NSF" is the National Science Foundation (https://www.nsf.gov/). The work in Tice and Song was funded by US Government funding, i.e., public monies (see also https://www.nsf.gov/funding/pgm_summ.jsp?pims_id=5295, explaining the NSF funding of MRSECs).

The work in Tice and Song is also the work in the Ismagilov patents, representative of which is US Patent No. 8,889,083, ("the '083 patent"), one of the patents-in-suit. The inventors named on the '083 patent overlap with the authors on Song and Tice, e.g., all of Ismagilov, Tice and Song are named co-inventors on the '083 patent and named co-authors on Song and Tice. All of Song, Tice and the '083 patent address control of multiple reactions in microfluidic systems (*see, e.g.*, Song at p. 768; Tice at 9127; '083 patent at Background). For ease of comparison, the following table, using the illustrations from Song, Tice and the '083 patent, shows that the technology of the '083 patent is the same as that which is disclosed in Song and Tice and thus that the technology in the '083 patent was developed using Government funding or public monies.

<table>
<tr><th colspan="2">COMPARISON OF I. SONG AND TICE AND II. THE '083 PATENT</th></tr>
<tr><th>I. SONG AND TICE</th><th>II. THE '083 PATENT</th></tr>
<tr><td>Figure 1a from Song et al. shows a standard pressure-driven microfluidic system, characterized by slow mixing and high dispersion of aqueous input streams.

Figure 1a from Tice et al. shows injection of aqueous streams into an immiscible fluid to form plugs in which reagents are rapidly mixed without dispersion.</td><td>Figure 2A of the '083 patent shows slow mixing and high dispersion (Fig. 2A-1) compared to injection of aqueous streams into an immiscible carrier to form plugs having rapid mixing and no dispersion (Fig. 2A-2).</td></tr>
<tr><td> 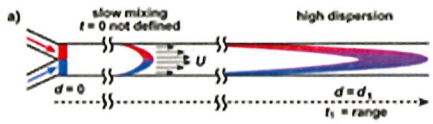

Song et al., Fig. 1a
 
Tice et al., Fig. 1a</td><td> 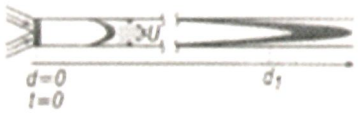

FIG. 2A-1
 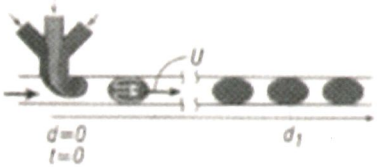

FIG. 2A-2</td></tr>
</table>

COMPARISON OF I. SONG AND TICE AND II. THE '083 PATENT (CONT.)	
I. SONG AND TICE	**II. THE '083 PATENT**
Figure 1b of Song shows changing channel geometries to control mixing.	Figure 5 of the '083 patent shows changing channel geometries to control mixing.
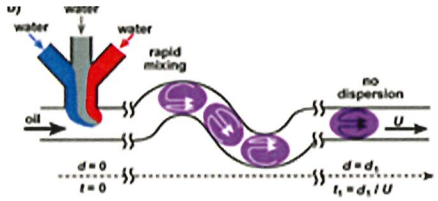 Song et al., Fig. 1b	 FIG. 5
Song, Figure 2 shows a schematic diagram of a microchannel network with flow rates, and photomicrographs of plug formation and transport.	Figure 5 of the '083 patent shows a schematic diagram of a microchannel network and photomicrographs of plug formation and transport. Flow rates are set forth in the specification.
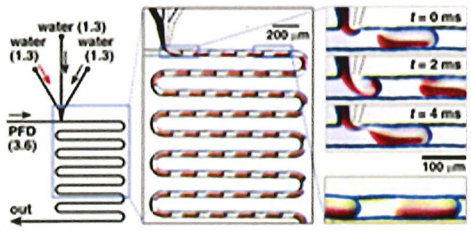 Fig. 2	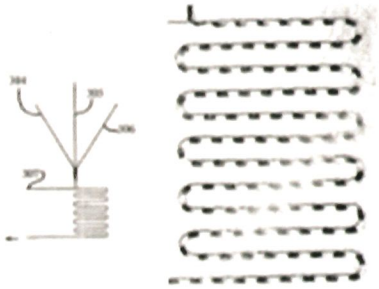 FIG. 3

COMPARISON OF I. SONG AND TICE AND II. THE '083 PATENT (CONT.)	
I. SONG AND TICE	**II. THE '083 PATENT**
Song, Fig. 4 shows rapid mixing inside plugs (Fig. 4a) and negligible mixing in a laminar flow (Fig. 4b). Fig. 4c shows fluorescence obtained by plug formation and mixing of reagents in the plug, and Fig. 4d shows the reaction proceeds as a function of time (left) or distance traveled by the plugs (right). Figure 4e shows weak fluorescence arising from negligible mixing in a laminar flow.	Figure 7 of the '083 patent shows rapid mixing inside plugs (a) and negligible mixing in a laminar flow (b). Fig. 7c shows fluorescence obtained by plug formation and mixing of reagents in the plug, and Fig. 7d shows the reaction proceeds as a function of time (left) or distance traveled by the plugs (right). Figure 7e shows weak fluorescence arising from negligible mixing in a laminar flow
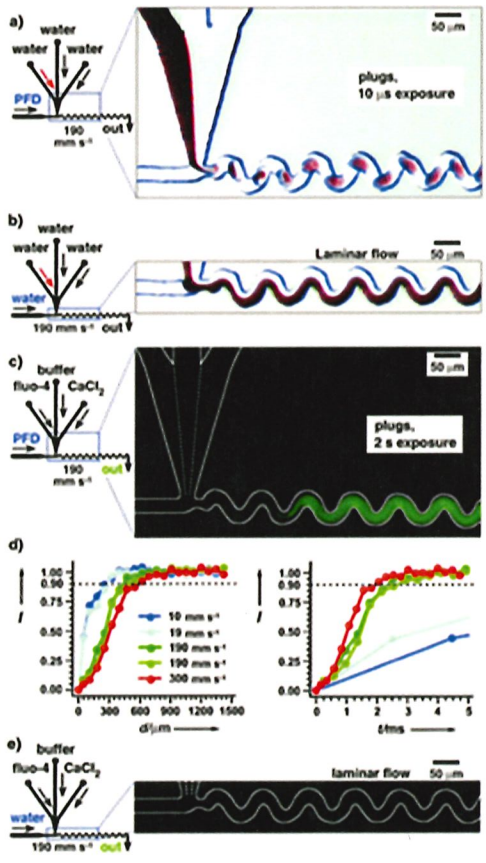 Fig. 4	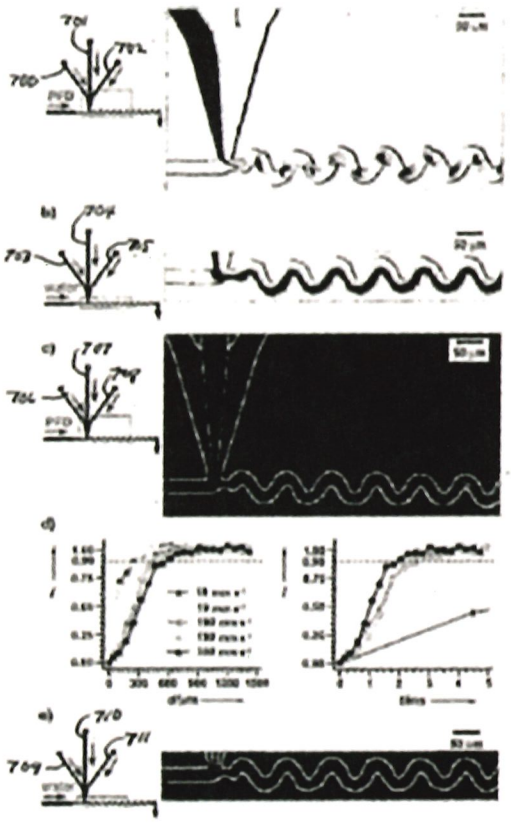 FIG. 7

COMPARISON OF I. SONG AND TICE AND II. THE '083 PATENT (CONT.)	
I. SONG AND TICE	**II. THE '083 PATENT**
Song, Fig. 5a shows a schematic diagram for spontaneous merging of plugs and a photomicrograph of two streams of plugs merging in a main channel. Fig. 5b shows a schematic diagram for spontaneous splitting of plugs at a branching point and photomicrographs of plugs splitting into volumes approximately one-half the volume of the initial plug or asymmetric splitting where outlet pressures are not equal.	Figure 33b of the '083 patent shows a schematic diagram for spontaneous merging of plugs and a photomicrograph of two streams of plugs merging in a main channel. Fig. 34a-c shows a schematic diagram for spontaneous splitting of plugs at a branching point and photomicrographs of plugs splitting into volumes approximately one-half the volume of the initial plug or asymmetric splitting where outlet pressures are not equal.
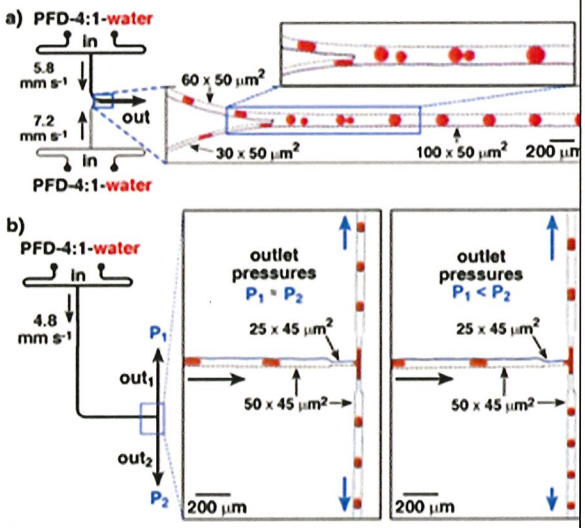 Fig. 5	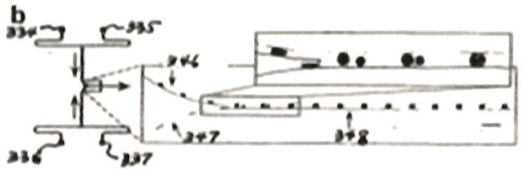 Fig. 33b 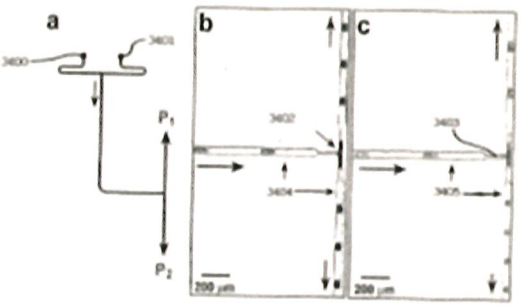 FIGS. 34a-c

It is therefore respectfully asserted that there is a key fact that does not seem to have been brought to the Court's attention, namely, that US public monies, i.e., US Government funding, was used to develop the patent subject matter at issue in the subject litigation.

It is further respectfully asserted that since US Government funding (US public monies) was used to develop patents-in-suit, and these patents are for research tools that are necessary for

Broad and NIH public interest research (including such research as discussed herein), the patents-in-suit should not be used by Bio-Rad to restrict the ability of the public, as represented by academic and/or not-for-profit research organizations, such as Broad, MIT, Harvard, the Harvard-affiliated hospitals, and Broad's collaborators (including the NIH) to use and to continue to use those research tools. Quite simply, as an equitable matter, the US Government funding dictates that the tools developed by that funding, i.e., the subject matter of the patents-in-suit, be made available for use by the public; and, that to do so means that the Court should not grant any permanent injunction as to 10X's products.

By allowing the single-cell genomics technology at issue in the subject litigation, including as embodied in 10X's products, to continue to be available at least to academics and/or not-for-profits as requested herein (i.e., without immediate and broad injunction), the Court will prevent serious setbacks in biomedical research and thereby advance the public interest. And, of course, the public interest is one of the reasons that injunctions are available in certain circumstances and not available in others as well as public interest informing any appropriate ongoing royalty. Here, for the ongoing projects of academic and research institutions and other not-for-profit activities, injunctions that limit or destroy the ability to conduct such research (especially when the patented technology at issue has, at least in part, been the fruits of US public funds/US Government grants), are contrary to the public interest.

Further, by not entering an immediate and broad injunction on instruments and reagents and so allowing research to continue, Broad submits that the Court will pave the way for all parties (not just the litigants here) in the single-cell genomics space to join together, thereby enabling robust development of technology in this space. Broad is available to work with 10X and Bio-Rad and other academic and commercial parties and patent holders to come together and

collectively work together to create a pool through which patent barriers to using single-cell genomics technology may be removed as to academics and/or not-for profits, so that academics and/or not-for profits have unfettered access to these necessary tools for biomedical research while still recognizing the need for patents as an important reward for the risks of research. As an additional benefit to the parties, the public and the Courts, not entering an immediate and broad injunction and so allowing research to continue could also result in a reduction of patent litigation around single-cell genomics technologies, and advance the interests of justice.

Accordingly, the Court, by adopting Broad's suggestion of there being no immediate and broad injunction (nor onerous royalty rate for academic and research use), especially for US Government funded or spearheaded projects, will be advancing the public interest and the interests of justice, and such a position by the Court will be consistent with the US Government funding (US public monies) that were utilized in the development of patents-in-suit.

B. Single Cell Technologies are Important to Advances in Human Health

The single cell technologies involved here are clearly important to research that will result in advances of the care of humans, and aid in understanding of the complexity of biological networks and organisms, human and non-human. Science Magazine has chosen single-cell genomics as the 2018 Breakthrough of the Year (*see* Pennisi, "Development Cell-by-Cell," Science 362(6421): 1344-1345 (21 Dec 2018), DOI: 10.1126/science.362.6421.1344, a copy provided herewith as Exhibit A)—technology understood to be at the heart of the issues before the Court—this technology enables the goal of the Human Cell Atlas Project to be within reach. As noted in the Science article cited above, it is a combination of techniques that have converged to initiate the single cell revolution, many of which have origins with US Government funded research, especially in academic and non-profit research institutions, including Broad with early and frequent advances for devices, tools and methods to label, perturb, measure and

analyze cells individually and in tissues and to tease apart what makes them work properly, so that humanity might understand diseases and disorders.

As noted in the January 2, 2019 NIH Director's Blog by Dr. Francis Collins highlighting biomedical advances in 2018, https://directorsblog.nih.gov/author/collinsfs/ (a copy provided herewith as Exhibit B, hyperlinks removed from below quote, underlining in original at hyperlinks),

> The 2018 Breakthrough of the Year went to biomedical science and its ability to track the development of life—one cell at a time—in a variety of model organisms. This newfound ability opens opportunities to understand the biological basis of life more systematically than ever before. Among *Science's* "runner-up" breakthroughs, more than half had strong ties to the biomedical sciences and NIH-supported research.
>
> Sound intriguing? Let's take a closer look at some of the amazing science conducted in 2018, starting with *Science's* Breakthrough of the Year.
>
> **Development Cell by Cell**: For millennia, biologists have wondered how a single cell develops into a complete multicellular organism, such as a frog or a mouse. But solving that mystery was almost impossible without the needed tools to study development systematically, one cell at a time. That's finally started to change within the last decade. I've highlighted the emergence of some of these powerful tools on my blog and the interesting ways that they were being applied to study development.
>
> Over the past few years, all of this technological progress has come to a head. Researchers, many of them NIH-supported, used sophisticated cell labeling techniques, nucleic acid sequencing, and computational strategies to isolate thousands of cells from developing organisms, sequence their genetic material, and determine their location within that developing organism.
>
> In 2018 alone, groundbreaking single-cell analysis papers were published that sequentially tracked the 20-plus cell types that arise from a fertilized zebrafish egg, the early formation of organs in a frog, and even the creation of a new limb in the Axolotl salamander. This is just the start of amazing discoveries that will help to inform us of the steps, or sometimes missteps, within human development—and suggest the best ways to prevent the missteps. In fact, efforts are now underway to gain this detailed information in people, cell by cell, including the international Human Cell Atlas and the NIH-supported Human BioMolecular Atlas Program.

Important planned and ongoing research performed will be directly impacted by the Court's decisions on the issues before it, especially the existence and scope of any permanent injunction and/or the level of ongoing royalties.

Huge data projects are currently focused on developing the cell based data necessary for important advances in human health. For example, the NCI Human Tumor Atlas Network, a part of the Cancer Moonshot[SM], is a US government project that uses such genomics. This is a major NIH project that involves fresh tumor samples from human patients that must be processed immediately and in a cost-effective manner. These initiatives require much data to be collected from many human samples. Use of the single-cell genomics at issue in the subject litigation, by Broad, NIH and others was envisioned by the Program seeking to improve the ability to understand and treat disease. (See, e.g., https://www.cancer.gov/research/key-initiatives/moonshot-cancer-initiative/implementation/human-tumor-atlas and https://www.cancer.gov/research/key-initiatives/moonshot-cancer-initiative, copies provided herein, in part, as Exhibits C and D).

Like projects pre-single cell data, these initiatives are expected to have a huge impact. As noted in the January 3, 2019 Science News, "Huge trove of British biodata is unlocking secrets of depression, sexual orientation, and more", https://www.sciencemag.org/news/2019/01/huge-trove-british-biodata-unlocking-secrets-depression-sexual-orientation-and-more, (a copy provided herewith as Exhibit E:

> In 2015, his team released the first batch of genetic data on a subset of 150,000 participants. Then came the July 2017 release of full genotyping data for all 500,000. Two months later, Benjamin Neale's group at the Broad Institute put up its blog doubling the number of markers linked to traits and disorders, as well as a web browser for looking up specific markers. "We viewed it as a service to the community," Neale says.
>
> Today, about 7000 researchers have registered to use UKB data on 1400 projects, and nearly 600 papers have been published. Some studies simply link

> behaviors and disease, for example reporting that drinking more coffee can reduce mortality but that binge-watching TV is associated with more colon cancer. But most studies compare the genomes of people with some trait or disease with those without it, in order to home in on genes that influence that attribute; these projects are known as genome-wide association studies.
>
> The result, every few days, is a new paper using UKB data to link particular gene variants to a disease or trait—arthritis, type 2 diabetes, depression, neuroticism, heart disease. "It's so easy for people who don't collect their own data," says statistical geneticist Danielle Posthuma of Vrije University in Amsterdam, who studies brain diseases. By combining data from the UKB and other collections, investigators can amass samples of a million people or more, amplifying the signal of gene variants with subtle effects. For some diseases, dozens or hundreds of genes appear to play a role. The genetic links are suggestive correlations; establishing cause and effect will take more genetics work and lab studies, which could reveal new disease pathways that might be drug targets.

This success is largely because of the amount of data that has been amassed and made public.

Today, many current data collection efforts are ongoing based on single cell technologies. As showcased on January 5, 2019 on National Public Radio, "Biological Cartographers Seek To Map The Trillions Of Cells In The Human Body", https://www.npr.org/2019/01/05/682394195/biological-Cartographers-seek-to-map-the-trillions-of-cells-in-the-human-body, (a copy provided herewith as Exhibit F), current efforts are underway, using these technologies, to map the around 37 trillion cells in the human body. In so doing, scientists are now relying on powerful single cell technology with high throughput at a reasonable cost to discover the kinds of cells that weren't previously recognized.

The ability to access technologies of the work plan and the price of such access are key drivers of success. If price is prohibitive or access is restricted, increased costs require creative partnering with commercial parties, often delaying release of data, or reduction in data—as well as delay in delivery to the world of treatments and therapies. Given the complex diseases and disorders (and concomitant treatments and therapies) this vast amount of data may be able to unlock, the public interest weighs strongly in favor of a solution that allows ongoing projects to

continue efficiently, while providing incentive to technology producers to work together and with academic and non-profit partners to ensure that suitable technology is available.

C. Subject Litigation Technology Not Fungible

The single-cell genomics technology of 10X's products is not fungible with the offerings of other manufacturers nor can it be readily replaced by Broad, MIT, Harvard, the Harvard-affiliated hospitals, and Broad's collaborators (including the NIH).

As shown by the data in Ding et al., "Progress Towards a Systematic Comparison of Single Cell RNA-Seq Methods", poster, a copy as presented publicly is provided herewith, as Exhibit G), the machines and methods are different, and 10X provides a benchmarked solution optimizing parameters for high throughput uses now surpassing Broad's Drop Seq technology as was showcased in 2013.

For ongoing projects with existing data, there needs to be the ability to continue use of the same instruments, i.e., 10X instruments, and reagents and with optimized protocols specific thereto by Broad and others in order to retain the value of the existing data, results obtained as to other instruments and other reagents will likely not be able to be readily comparable. To require that Broad and others switch to other instruments immediately and in the middle of projects means that previous research work on those projects likely will need to be discarded and the work redone on new instruments and with new reagents after time taken to learn and optimize protocols specific for the new instruments and new reagents in order to have the needed consistency. And, during this period of changeover and re-optimization, precious biological samples (especially from humans) may be lost as they will not be able to be timely used.

Moreover, if such a switch is required and even if the project is such that the work can be re-done, Broad and other research institutions have no means to recover the monetary costs of re-doing research work. Thus, if called upon to so do based on an injunction order by the Court,

Broad and others, and therefore the public, will be irreparably harmed (e.g., because laboratory time and space would be devoted to re-doing past work rather than advancing ongoing research and hence no amount of money can compensate for the losses). It is not possible to simply exchange the 10X machine with that of Bio-Rad as "similar data" on different systems is not generally accepted as equivalent for the purposes of research projects of the type at issue here.

If indeed Bio-Rad introduces an even more robust system that leapfrogs 10X system in performance (as indicated by Bio-Rad), that new platform will be able to compete in the marketplace for new projects and further uses as the metrics are established and protocols optimized for droplet applications and single cell processing. This future adoption of supposedly superior instruments will not be advanced by derailing ongoing projects or unnecessary re-commitment of funds to buy other systems available today. This future adoption will succeed on its own merits.

It is earnestly asserted that an immediate injunction will cause irreparable harm, including because the single-cell genomics technologies are not interchangeable; not fungible.

Many publicly supported advances are reflected in any working system, and those elements need to be combined to enable the progress necessary to address today's complex challenges. A patent pool would enable such cross licensing and co-development opportunities to emerge. This Court will pave the way for these parties and those in single-cell genomics space to join together by allowing all sales of the infringing products to continue, at least for academic and non-profit research use and as part of ongoing US Government funded projects.

III. Conclusion

The Court, by adopting Broad's suggestion of there being no immediate injunction, and no onerous royalty rate for research by academic and not-for-profit institutions, especially on reagents, will be advancing the public interest and the interests of justice, by preventing

irreparable harm to Broad and other similarly-situated institutions (including those identified in the Broad *Amicus Curiae* Motion), and by advancing necessary and critical biomedical research that is ongoing. In the same way, while Broad realizes the need in normal circumstances for payment to the owners of valid patent claims to technology that is being used, the royalty in situations such as the present one must be set at fair rate that will not raise the price to a degree where it is the economic equivalent of an injunction.

Broad respectfully requests that, in view of the information provided herein and in the Broad *Amicus Curiae* Motion, there be no immediate injunction imposed by the Court that precludes use of 10X technology, particularly by academic and not-for-profit institutions.

Respectfully submitted,

January 9, 2019

DUANE MORRIS LLP

/s/Richard L. Renck

Richard L. Renck (#3893)
222 Delaware Avenue, Suite 1600Wilmington, DE 19801Telephone: (302) 657-4900Fax: (302) 657-4901
rlrenck@duanemorris.com

Counsel for non-party, The Broad Institute, Inc.

Of Counsel:

Thomas J. Kowalski, Esq.
Duane Morris LLP
1540 Broadway
New York, NY 10036-4086
Telephone: (212) 692-1025
Fax: (212) 202-7805
TJKowalski@duanemorris.com

EXHIBIT A

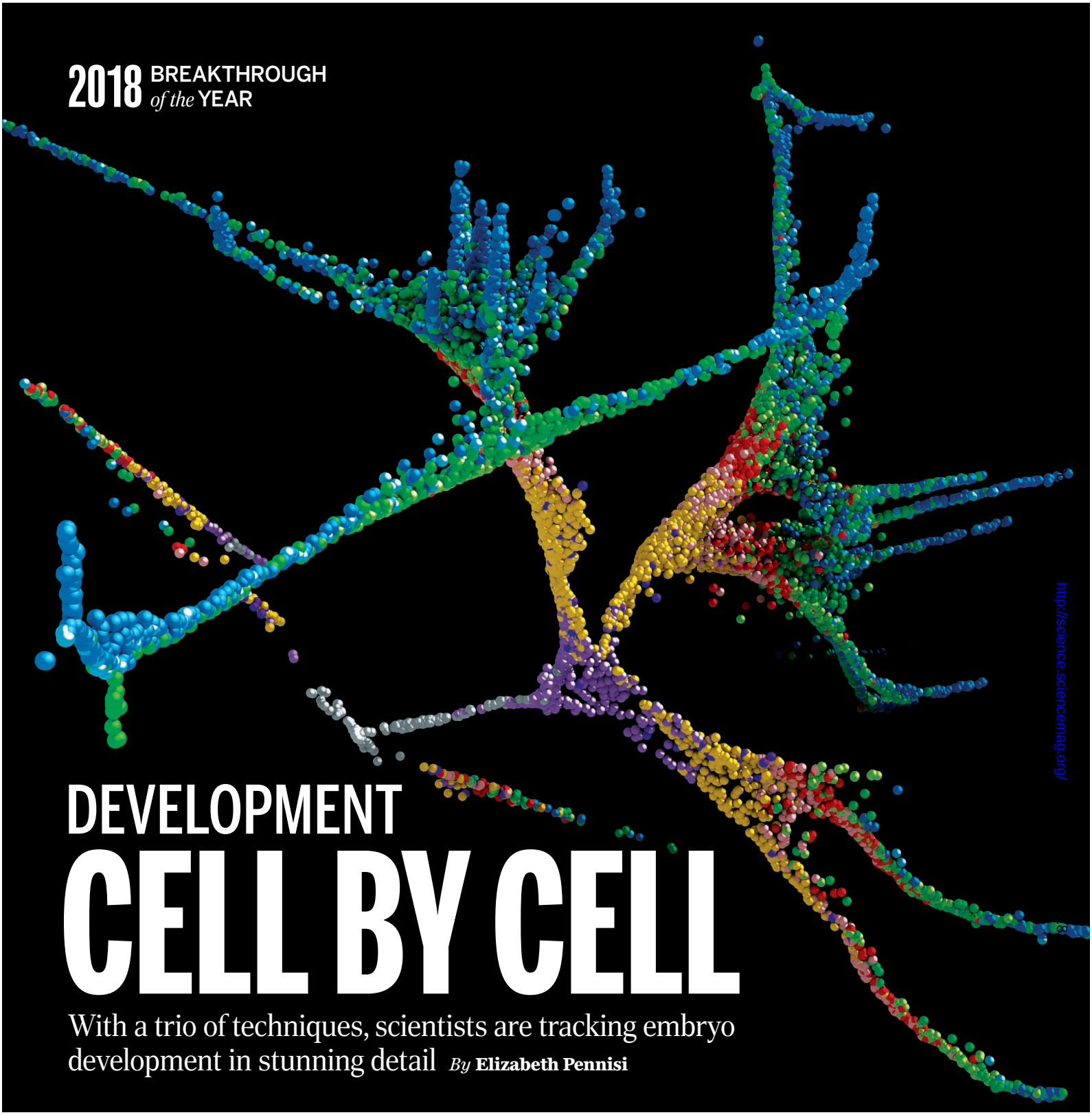

DEVELOPMENT
CELL BY CELL

With a trio of techniques, scientists are tracking embryo development in stunning detail *By* **Elizabeth Pennisi**

From at least the time of Hippocrates, biologists have been transfixed by the mystery of how a single cell develops into an adult animal with multiple organs and billions of cells. The ancient Greek physician hypothesized that moisture from a mother's breath helps shape a growing infant, but now we know it is DNA that ultimately orchestrates the processes by which cells multiply and specialize. Now, just as a music score indicates when strings, brass, percussion, and woodwinds chime in to create a symphony, a combination of technologies is revealing when genes in individual cells switch on, cueing the cells to play their specialized parts. The result is the ability to track development of organisms and organs in stunning detail, cell by cell and through time. *Science* is recognizing that combination of technologies, and its potential for spurring advances in basic research and medicine, as the 2018 Breakthrough of the Year.

Driving those advances are techniques for isolating thousands of intact cells from living organisms, efficiently sequencing expressed genetic material in each cell, and

IMAGE: JEFFREY FARRELL AND YIQUN WANG/SCHIER LAB/HARVARD UNIVERSITY

Published by AAAS

A representation of cell lineages in a zebrafish embryo, color-coded by time. The first cells are gray; by 6 hours (gold), three major branches have formed.

using computers, or labeling the cells, to reconstruct their relationships in space and time. That technical trifecta "will transform the next decade of research," says Nikolaus Rajewsky, a systems biologist at the Max Delbrück Center for Molecular Medicine in Berlin. This year alone, papers detailed how a flatworm, a fish, a frog, and other organisms begin to make organs and appendages. And groups around the world are applying the techniques to study how human cells mature over a lifetime, how tissues regenerate, and how cells change in diseases.

ON OUR WEBSITE

For more on the Breakthrough of the Year, including a video and a podcast, go to: https://scim.ag/Breakthrough2018

The ability to isolate thousands of individual cells and sequence each one's genetic material gives researchers a snapshot of what RNA is being produced in each cell at that moment. And because RNA sequences are specific to the genes that produced them, researchers can see which genes are active. Those active genes define what a cell does.

That combination of techniques, known as single-cell RNA-seq, has evolved over the past few years. But a turning point came last year, when two groups showed it could be done on a scale large enough to track early development. One group used single-cell RNA-seq to measure gene activity in 8000 cells extracted at one time point from fruit fly embryos. About the same time, another team profiled gene activity of 50,000 cells from one larval stage of the nematode *Caenorhabditis elegans*. The data indicated which proteins, called transcription factors, were guiding the cells to differentiate into specialized types.

This year, those researchers and others performed even more extensive analyses on vertebrate embryos. Using a variety of sophisticated computational methods, they linked single-cell RNA-seq readouts taken at different time points to reveal the turning on and off of sets of genes that defined the types of cells formed in those more complex organisms. One study uncovered how a fertilized zebrafish egg gives rise to 25 cell types; another monitored frog development through early stages of organ formation and determined that some cells begin to specialize earlier than previously thought. "The techniques have answered fundamental questions regarding embryology," says Harvard University stem cell biologist Leonard Zon.

Researchers interested in how some animals can regrow limbs or whole bodies have also turned to single-cell RNA-seq. Two groups studied gene expression patterns in aquatic flatworms called planaria—among biology's champion regenerators—after they had been cut into pieces. The scientists discovered new cell types and developmental trajectories that emerged as each piece regrew into a whole individual. Another group traced the genes that switched on and off in axolotls, a type of salamander, that had lost a forelimb. The researchers found that some mature limb tissue reverted to an embryonic, undifferentiated state and then underwent cellular and molecular reprogramming to build a new limb.

Because cells must be removed from an organism for single-cell sequencing, that technique alone can't show how those cells interact with their neighbors or identify the cells' descendants. But by engineering markers into early embryonic cells, researchers can now track cells and their progeny in living organisms. At least one team exposes early embryos to mobile genetic elements that carry genes for different colored fluorescent tags, which randomly settle into the cells, imparting different colors to each cell lineage. Other teams have harnessed the gene-editing technique called CRISPR to mark the genomes of individual cells with unique barcodelike identifiers, which are then passed on to all their descendants. The gene editor can make new mutations in progeny cells while retaining the original mutations, enabling scientists to track how lineages branch off to form new cell types.

By combining those techniques with single-cell RNA-seq, researchers can both monitor the behavior of individual cells and see how they fit into the organism's unfolding architecture. Using that approach, one team determined the relationships of more than 100 cell types in zebrafish brains. The researchers used CRISPR to mark early embryonic cells, then isolated and sequenced 60,000 cells at different time points to track gene activity as the fish embryo developed.

Other groups are applying similar techniques to track what happens in developing organs, limbs, or other tissues—and how those processes can go wrong, resulting in malformations or disease. "It's like a flight recorder, where you are watching what went wrong and not just looking at a snapshot at the end," says Jonathan Weissman, a stem cell biologist at the University of California, San Francisco. "We can ask questions at a resolution that was just not possible before."

Although those technologies cannot be used directly in developing human embryos, researchers are applying the approaches to human tissues and organoids to study gene activity cell by cell and characterize cell types. An international consortium called the Human Cell Atlas is 2 years into an effort to identify every human cell type, where each type is located in the body, and how the cells work together to form tissues and organs. Already, one project has identified most, if not all, kidney cell types, including ones that tend to become cancerous. Another effort has revealed the interplay between maternal and fetal cells that allows pregnancy to proceed. And a collaboration of 53 institutions and 60 companies across Europe, called the LifeTime consortium, is proposing to harness single-cell RNA-seq in a multipronged effort to understand what happens cell by cell as tissues progress toward cancer, diabetes, and other diseases.

High-resolution movies of development and disease will only get more compelling. Papers already posted online extend development studies to ever-more-complex organisms. And researchers hope to combine single-cell RNA-seq with new microscopy techniques to see where in each cell its distinctive molecular activity takes place and how neighboring cells affect that activity.

The single-cell revolution is just starting. ■

PEOPLE'S CHOICE

Our readers weigh in with their picks for the top breakthrough of 2018

Visitors to *Science*'s website are in agreement with the magazine's reporters and editors: Development cell by cell is the Breakthrough of the Year.

We invited online readers to vote on a dozen candidates for the breakthrough. The first round of voting narrowed the choices to four, and a second round, in which more than 12,000 votes were cast, determined the top People's Choice.

The combination of techniques that enables scientists to track development at the cellular level, in stunning detail and over time, was the clear winner. The approval of a gene-silencing drug after 20 years of development took second place, followed by the detection of a neutrino traced to a source outside our galaxy. The fourth contender, a set of images of the fruit fly brain showing individual synapses, just missed *Science*'s top 10.

1. Development cell by cell **35%**
2. RNAi drug approved **30%**
3. Neutrinos from a blazar **23%**
4. Fly brain revealed **12%**

Science

Development cell by cell

Elizabeth Pennisi

Science **362** (6421), 1344-1345.
DOI: 10.1126/science.362.6421.1344

EXHIBIT B

NIH Director's Blog

Search The Blog

Biomedical Research Highlighted in Science's 2018 Breakthroughs

Posted on January 2nd, 2019 by Dr. Francis Collins

A Happy New Year to one and all! While many of us were busy wrapping presents, the journal *Science* announced its much-anticipated scientific breakthroughs of 2018. In case you missed the announcement [1], it was another banner year for the biomedical sciences.

The 2018 Breakthrough of the Year went to biomedical science and its ability to track the development of life—one cell at a time—in a variety of model organisms. This newfound ability opens opportunities to understand the biological basis of life more systematically than ever before. Among *Science's* "runner-up" breakthroughs, more than half had strong ties to the biomedical sciences and NIH-supported research.

Sound intriguing? Let's take a closer look at some of the amazing science conducted in 2018, starting with *Science's* Breakthrough of the Year.

Development Cell by Cell: For millennia, biologists have wondered how a single cell develops into a complete multicellular organism, such as a frog or a mouse. But solving that mystery was almost impossible without the needed tools to study development systematically, one cell at a time. That's finally started to change within the last decade. I've highlighted the emergence of some of these powerful tools on my blog and the interesting ways that they were being applied to study development.

Over the past few years, all of this technological progress has come to a head. Researchers, many of them NIH-supported, used sophisticated cell labeling techniques, nucleic acid sequencing, and computational strategies to isolate thousands of cells from developing organisms, sequence their genetic material, and determine their location within that developing organism.

In 2018 alone, groundbreaking single-cell analysis papers were published that sequentially tracked the 20-plus cell types that arise from a fertilized zebrafish egg, the early formation of organs in a frog, and even the creation of a new limb in the Axolotl salamander. This is just the start of amazing discoveries that will help to inform us of the steps, or sometimes missteps, within human development—and suggest the best ways to prevent the missteps. In fact, efforts are now underway to gain this detailed information in people, cell by cell, including the international Human Cell Atlas and the NIH-supported Human BioMolecular Atlas Program.

An RNA Drug Enters the Clinic: Twenty years ago, researchers Andrew Fire and Craig Mello showed that certain small, noncoding RNA molecules can selectively block genes in our cells from turning "on" through a process called RNA interference (RNAi). This work, for the which these NIH grantees received the 2006 Nobel Prize in Physiology or Medicine, soon sparked a wave of commercial interest in various noncoding RNA molecules for their potential to silence the expression of a disease-causing gene.

After much hard work, the first gene-silencing RNA drug finally came to market in 2018. It's called Onpattro™ (patisiran), and the drug uses RNAi to treat the peripheral nerve disease that can afflict adults with a rare disease called hereditary transthyretin-mediated amyloidosis. This hard-won success may spark further development of this novel class of biopharmaceuticals to treat a variety of conditions, from cancer to cardiovascular disorders, with potentially greater precision.

Rapid Chemical Structure Determination: Last October, two research teams released papers almost simultaneously that described an incredibly fast new imaging technique to determine the structure of smaller organic chemical compounds, or "small molecules" at atomic resolution. Small molecules are essential components of molecular biology, pharmacology, and drug development. In fact, most of our current medicines are small molecules.

News of these papers had many researchers buzzing, and I highlighted one of them on my blog. It described a technique called microcrystal electron diffraction, or MicroED. It enabled these NIH-supported researchers to take a powder form of small molecules (progesterone was one example) and generate high-resolution data on their chemical structures in less than a half-hour! The ease and speed of MicroED could revolutionize not only how researchers study various disease processes, but aid in pinpointing which of the vast number of small molecules can become successful therapeutics.

How Cells Marshal Their Contents: About a decade ago, researchers discovered that many proteins in our cells, especially when stressed, condense into circumscribed aqueous droplets. This so-called phase separation allows proteins to gather in higher concentrations and promote reactions with other proteins. The NIH soon began supporting several research teams in their groundbreaking efforts to explore the effects of phase separation on cell biology.

Over the past few years, work on phase separation has taken off. The research suggests that this phenomenon is critical in compartmentalizing chemical reactions within the cell without the need of partitioning membranes. In 2018 alone, several major papers were published, and the progress already has some suggesting that phase separation is not only a basic organizing principle of the cell, it's one of the major recent breakthroughs in biology.

Forensic Genealogy Comes of Age: Last April, police in Sacramento, CA announced that they had arrested a suspect in the decades-long hunt for the notorious Golden State Killer. As exciting as the news was, doubly interesting was how they caught the accused killer. The police had the Golden Gate Killer's DNA, but they couldn't determine his identity, that is, until they got a hit on a DNA profile uploaded by one of his relatives to a public genealogy database.

Though forensic genealogy falls a little outside of our mission, NIH has helped to advance the gathering of family histories and using DNA to study genealogy. In fact, my blog featured NIH-supported work that succeeded in crowdsourcing 600 years of human history.

The researchers, using the online profiles of 86 million genealogy hobbyists with their permission, assembled more than 5 million family trees. The largest totaled more than 13 million people! By merging each tree from the crowd-sourced and public data, they were able to go back about 11 generations—to the 15th century and the days of Christopher Columbus. Though they may not have caught an accused killer, these large datasets provided some novel insights into our family structures, genes, and longevity.

An Ancient Human Hybrid: Every year, researchers excavate thousands of bone fragments from the remote Denisova Cave in Siberia. One such find would later be called Denisova 11, or "Denny" for short.

Oh, what a fascinating genomic tale Denny's sliver of bone had to tell. Denny was at least 13 years old and lived in Siberia roughly 90,000 years ago. A few years ago, an international research team found that DNA from the mitochondria in Denny's cells came from a Neanderthal, an extinct human relative.

In 2018, Denny's family tree got even more interesting. The team published new data showing that Denny was female and, more importantly, she was a first generation mix of a Neanderthal mother and a father who belonged to another extinct human relative called the Denisovans. The Denisovans, by the way, are the first human relatives characterized almost completely on the basis of genomics. They diverged from Neanderthals about 390,000 years ago. Until about 40,000 years ago, the two occupied the Eurasian continent—Neanderthals to the west, and Denisovans to the east.

Denny's unique genealogy makes her the first direct descendant ever discovered of two different groups of early humans. While NIH didn't directly support this research, the sequencing of the Neanderthal genome provided an essential resource.

As exciting as these breakthroughs are, they only scratch the surface of ongoing progress in biomedical research. Every field of science is generating compelling breakthroughs filled with hope and the promise to improve the lives of millions of Americans. So let's get started with 2019 and finish out this decade with more truly amazing science!

Reference:

[1] "2018 Breakthrough of the Year ," Science, 21 December 2018.

NIH Support: These breakthroughs represent the culmination of years of research involving many investigators and the support of multiple NIH institutes.

Related

Happy New Year … and a Look Back at a Memorable 2015
January 5, 2016
In "Health"

What a Year It Was! A Look Back at Research Progress in 2017
January 2, 2018
In "Health"

NIH-Funded Research Makes Science's "Top 10" List
January 6, 2015
In "Health"

Posted In: News

Tags: 2018 Breakthrough of the Year, Andrew Fire, axolotl salamander, biopharmaceuticals, cell biology, Craig Mello, Denisovans, developmental biology, forensic genealogy, frog, genome, hereditary transthyretin-mediated amyloidosis, Human Cell Atlas, MicroED, Neanderthals, Nobel Prize, noncoding RNA, Onpatrro, patisiran, phase separation, rare disease, RNA, RNA interference, RNAi, Science's Breakthroughs of the Year, single cell analysis, small molecules, zebrafish

3 Comments

john liposky **says:**
January 2, 2019 at 1:57 pm
Stem cell treatment for arthritis should be at the head of Century 21 Cures act. Lots of phase 1 & 2 show only positive results which should promise Phase 3 & 4 Clinical Trials with disappointing expectations from all potential researchers. With 75 million Americans suffering, this treatment offers the biggist cost saving and pain elimination for a condition that has no other cure.

Reply

Víctor **says:**
January 3, 2019 at 4:09 am
Happy New Year and a great greeting from Spain!

Reply

MARK RUSSELL **says:**
January 3, 2019 at 10:52 am
This research should be on the front page of every Newspaper in America. Instead of seeing the despair of what is wrong with society—why not see a bright future? What has been accomplished this year

from the NIH should be discussed at every dinner table in America. Every classroom from New York to Los Angeles, should know about the breakthroughs in all areas of Medicine. In 1969 we went to the moon——Why not cure all Cancers and why not increase our life Span by (20) years? I applaud the ground breaking research the NIH is taking.

Reply

Leave a Comment

Enter your comment here...

Recent Items

- Connecting Senescent Cells to Obesity and Anxiety January 8, 2019
- New NIBIB Director January 7, 2019
- Biomedical Research Highlighted in Science's 2018 Breakthroughs January 2, 2019
- 'Tis the Season for Good Cheer December 20, 2018
- 'Exercise Hormone' Tied to Bone-Strengthening Benefits December 18, 2018

Blog Archives

Select Month

About the NIH Director

Francis S. Collins, M.D., Ph.D.

Appointed the 16th Director of NIH by President Barack Obama and confirmed by the Senate. He was sworn in on August 17, 2009. On June 6, 2017. President Donald Trump announced his selection of Dr. Collins to continue to serve as the NIH Director.

More about Dr. Collins

@NIHDirector on Twitter

Senescent cells have been tied to a wide range of #health problems related to #aging. Are they behind #obesity-rela… https://t.co/u76Gf7zT38 **2 hours ago**

Just had the swearing in ceremony for new @NIBIBgov Director Dr. Bruce Tromberg this morning. Welcome to the #NIH f… https://t.co/zcVFGOj7fg **1 day ago**

A study found cells in the gut produce antibodies that migrate to the brain to reduce inflammation during MS flare-… https://t.co/mQIfO57SsH **3 days ago**

Follow @NIHDirector

NIH On Facebook

Follow on Facebook

Blog Info

Editor

Kendall Morgan, Ph.D.

Comments and Questions

If you have comments or questions not related to the current discussions, please direct them to **Ask NIH**.

You are encouraged to share your thoughts and ideas. Please review the **NIH Comments Policy**

EXHIBIT C

NIH NATIONAL CANCER INSTITUTE

Generation of Human Tumor Atlases

Cancer development, progression, and metastasis require complex interactions within the local tumor microenvironment that are mediated by many factors. Although researchers have made progress in understanding these interactions and their role in cancer processes, there are currently major knowledge gaps about the complete multidimensional architecture of tumors. In particular, little is known about how the biological composition and interactions within a tumor change over time and in response to cancer treatments.

NCI has announced several funding opportunities that align with the Cancer Moonshot.

See Funding Opportunities

This recommendation focuses on the generation of human tumor atlases that describe the various cellular, structural, and molecular characteristics of human cancers over time. Tumor atlases aim to characterize tumors from a diverse population of cancer patients and to describe tumor interactions with the microenvironment and the immune system, to help reveal the processes that underlie malignancy. Additionally, tumor atlases should map multiple stages in cancer ranging from precancerous lesions to advanced cancer metastasis.

The ultimate goal of this recommendation is to predict how cancers develop and respond to treatment in different populations, which will be used to assist researchers in developing new cancer treatments and strategies for cancer prevention.

NCI has awarded funding to the following research project that aligns with this recommendation's goal to generate human tumor atlases:

Human Tumor Atlas Network (HTAN)

HTAN is a collaborative network that is constructing 3-dimensional atlases of the cellular, morphological, molecular features of human cancers over time. There is a focus by the network on generating atlases representing a diverse cancer patient population and high-risk cancers. Additionally, the atlases being created by the network describe important transitions during cancer, such as the transition of pre-malignant cancers to malignant tumors, the progression to metastatic cancer, the response to cancer treatment, and the development of resistance to treatment.

The Human Tumor Atlas (HTA) Research Centers are focused on understanding the behaviors of advanced cancers in an organ-specific manner. The Pre-Cancer Atlas (PCA) Research Centers are focused on conditions that are likely to become cancer. The HTAN Data Coordinating Center manages the data storage, sharing, and compilation of the atlases constructed by the network.

The HTAN aims to represent a diverse patient population, including minority and underserved patients. Preference was given to pediatric and adult cancers that are highly metastatic, cancers that are promising candidates for immunotherapy or not responsive to immunotherapy, and high-risk hereditary tumors.

The comprehensive human tumor atlases that are being created by HTAN will accelerate the biological understanding of cancer and clinical decisions for the care of cancer patients.

Human Tumor Atlas Projects Awarded Cancer Moonshot Funding

Awarded Projects

Funding Opportunity	Project Title	Institution	Principal Investigator (s)
Human Tumor Atlas Network: Data Coordinating Center (U24)	Human Tumor Atlas Network: Data Coordinating Center	Dana-Farber Cancer Institute	Cerami, Ethan; Guinney, Justin; Reynolds, Sheila; Schultz, Nikolaus
Human Tumor Atlases (HTA) Precancer Atlas Research Centers (U2C)	Integrative Single-Cell Atlas of Host and Microenvironment in Colorectal Neoplastic Transformation	Vanderbilt University	Coffey, Robert J; Lau, Ken Siu Kwong; Shrubsole, Martha J
	Breast Pre-Cancer Atlas Center	Duke University	Hwang, Eun-Sil Shelley; Maley, Carlo; West, Robert B
	Precancer Atlas of Familial Adenomatous Polyposis	Stanford University	Snyder, Michael P; Ford, James M
	Pre-cancer Atlases of Cutaneous and Hematologic Origin (PATCH Center)	Harvard Medical School	Sorger, Peter Karl; Aster, Jon C; Santagata, Sandro
		Boston University Medical Campus	Spira, Avrum E; Dubinett, Steven M

Funding Opportunity	Project Title	Institution	Principal Investigator (s)
	The Lung PCA: A Multi-Dimensional Atlas of Pulmonary Premalignancy		
Human Tumor Atlases (HTA) Research Centers (U2C)	Washington University Human Tumor Atlas Research Center	Washington University	Ding, Li; Achilefu, Samuel; Fields, Ryan C; Gillanders, William E
	Omic and Multidimensional Spatial Atlas of Metastatic Breast and Prostate Cancers	Oregon Health & Science University	Gray, Joe W; Corless, Christopher L; Goecks, Jeremy; Mills, Gordon B
	The Cellular Geography of Therapeutic Resistance in Cancer	Dana-Farber Cancer Institute	Haining, William Nicholas; Regev, Aviv
	Transition to Metastatic State: Lung Cancer, Pancreatic Cancer and Brain Metastasis	Sloan-Kettering Institute for Cancer Research	Pe'er, Dana; Iacobuzio-Donahue, Christine A
	Center for Pediatric Tumor Cell Atlas	Children's Hospital of Philadelphia	Tan, Kai; Hunger, Stephen Patrick
National Cancer Institute Program Project Applications (P01)	Integrative Oncogenomics of Multiple Myeloma	Dana-Farber Cancer Institute	Munshi, Nikhil C

Posted: October 22, 2018

EXHIBIT D

NIH NATIONAL CANCER INSTITUTE

Cancer Moonshot℠

The Cancer Moonshot to accelerate cancer research aims to make more therapies available to more patients, while also improving our ability to prevent cancer and detect it at an early stage.

To ensure that the Cancer Moonshot's goals and approaches are grounded in the best science, a Cancer Moonshot Task Force consulted with external experts, including the presidentially appointed National Cancer Advisory Board (NCAB).

A Blue Ribbon Panel of experts was established as a working group of the NCAB to assist the board in providing this advice. The panel's charge was to provide expert advice on the vision, proposed scientific goals, and implementation of the Cancer Moonshot.

Get email updates from NCI on the Cancer Moonshot

Congress passed the 21st Century Cures Act in December 2016, authorizing $1.8 billion in funding for the Cancer Moonshot over 7 years. The funding must be appropriated each fiscal year over those 7 years. Congress appropriated $300 million to NCI for fiscal year (FY) 2017, $300 million for FY 2018, and $400 million for FY 2019.

Blue Ribbon Panel

A Blue Ribbon Panel of experts was established as a working group of the NCAB to ensure that the Cancer Moonshot's approaches are grounded in the best science. Their report outlines 10 recommendations to accelerate progress against cancer.

Cancer Moonshot℠ Research Initiatives

Implementation teams are considering multiple ways to fund new programs as well as expansions of ongoing efforts to advance the goals of the Cancer Moonshot.

Funding Opportunities to Support Cancer Moonshot

New Cancer Moonshot funding opportunities from NCI support goals articulated in the recommendations made by the Blue Ribbon Panel.

EXHIBIT E

UK Biobank Principal Investigator Rory Collins stands amid stored biospecimens from the project's half-million participants. NIGEL HILIER

Huge trove of British biodata is unlocking secrets of depression, sexual orientation, and more

By **Jocelyn Kaiser**, **Ann Gibbons** | Jan. 3, 2019 , 1:20 PM

In early 2017, epidemiologist Rory Collins at the University of Oxford in the United Kingdom and his team faced a test of their principles. They run the UK Biobank (UKB), a huge research project probing the health and genetics of 500,000 British people. They were planning their most sought-after data release yet: genetic profiles for all half-million participants. Three hundred research groups had signed up to download 8 terabytes of data—the equivalent of more than 5000 streamed movies. That's enough to tie up a home computer for weeks, threatening a key goal of the UKB: to give equal access to any qualified researcher in the world.

"We wanted to create a level playing field" so that someone at a big center with a supercomputer was at no more of an advantage than a postdoc in Scotland with a smaller computer and slower internet link, says Oxford's Naomi Allen, the project's chief epidemiologist. They came up with a plan: They gave researchers 3 weeks to download the encrypted files. Then, on 19 July 2017, they released a final encryption key, firing the starting gun for a scientific race.

Within a couple of days, one U.S. group had done quick analyses linking more than 120,000 genetic markers to more than 2000 diseases and traits, data it eventually put up on a blog. Only 60,000 markers had previously been tied to disease, says human geneticist Eric Lander, president and director of the Broad Institute in Cambridge, Massachusetts. "[They] doubled that in a week."

Within 2 weeks, others had begun to post draft manuscripts on the bioRxiv preprint site. By now, those data have spawned dozens of papers in journals or on bioRxiv, firming up how particular genes contribute to heart disease, diabetes, Alzheimer's, and other conditions, as well as genes' role in shaping personality, depression, birth weight, insomnia, and other traits. More controversially, data from the trove also pointed to DNA markers linked to education level and sexual orientation, stoking long-running controversies about the application of genetics to behavior in people.

Related story

Genetic data on half a million Brits reveal ongoing evolution and Neanderthal legacy

When the Manchester-based UKB enrolled its first volunteer 13 years ago, some critics wondered whether it would be a waste of time and money. But by now, any skepticism is long gone. "It's now clear that it has been a massive success—largely because the big data they have are being made widely available," says Oxford developmental neuropsychologist Dorothy Bishop, a participant. Other biobanks are bigger or collect equally detailed health data. But the UKB has both large numbers of participants and high-quality clinical information. It "allows us to do research on a scale that we've never been able to do before," says Peter Visscher, a quantitative geneticist at the University of Queensland in Brisbane, Australia.

The crucial ingredient, however, may be open access. Researchers around the world can freely delve into the UKB data and rapidly build on one another's work, resulting in unexpected dividends in diverse fields, such as human evolution. In a crowdsourcing spirit rare in the hypercompetitive world of biomedical research, groups even post tools for using the data without first seeking credit by publishing in a journal.

"The U.K. is getting all of the world's best brains" to study its citizens, says Ewan Birney, director of the EMBL European Bioinformatics Institute in Hinxton, U.K., and a member of the UKB's steering committee. The U.K. focus is also the project's chief downside, as it explores just one slice of humanity: northern Europeans. It holds data for only about 20,000 people of African or Asian descent, for example. Yet as new papers appear every few days, researchers say the UKB remains a shining example of the power of curiosity unleashed. "It's the thing we always dreamed of," Lander says.

> **"It's now clear that it has been a massive success—largely because the big data they have are being made widely available."**
>
> *Dorothy Bishop, University of Oxford*

The UKB was announced in the early 2000s as a classical epidemiological study—the kind used to associate risk factors such as diet and smoking with the development of disease over time. The model was the famous Framingham Heart Study, a long-term study that initially analyzed 5200 residents of Framingham, Massachusetts, seeking factors that influence heart disease. The UKB project, which has received $308 million in funding so far from the Wellcome Trust medical charity, the U.K. government, and disease foundations, "was going to be like Framingham, only 100 times bigger," says principal investigator Collins.

From 2006 to 2010, the UKB enrolled 500,000 people aged 40 to 69 through the United Kingdom's National Health Service. Mailed invitations were sent widely, including to people in poor and ethnically diverse areas of cities such as Birmingham. But in the end, participants were "anybody you could persuade," Collins says. Investigators sampled their blood and urine, surveyed their habits, and examined them for more than 2400 different traits or phenotypes, including data on their social lives, cognitive state, lifestyle, and physical health.

The blood samples yielded DNA for genomic analyses. Links to other U.K. databases added information such as cancer diagnoses, deaths, and hospitalizations. "If you're talking about common phenotypes, the Biobank shines," Lander says. "There's arm fat, smoking behavior, miserableness, neurotic behavior, time on your computer, eating behavior, drinking behavior."

Other biobanks have comparably rich health data, such as deCODE Genetics's detailed database on Iceland's population and biobanks run by U.S. health care providers. Some, such as the U.S. Million Veteran Program and the DNA testing company 23andMe, are bigger. But in most cases researchers can use these databases only by collaborating with their creators.

Engine of productivity

Published papers based on the UK Biobank's bounty of health and genetics data are piling up fast, in part because the data are freely available.

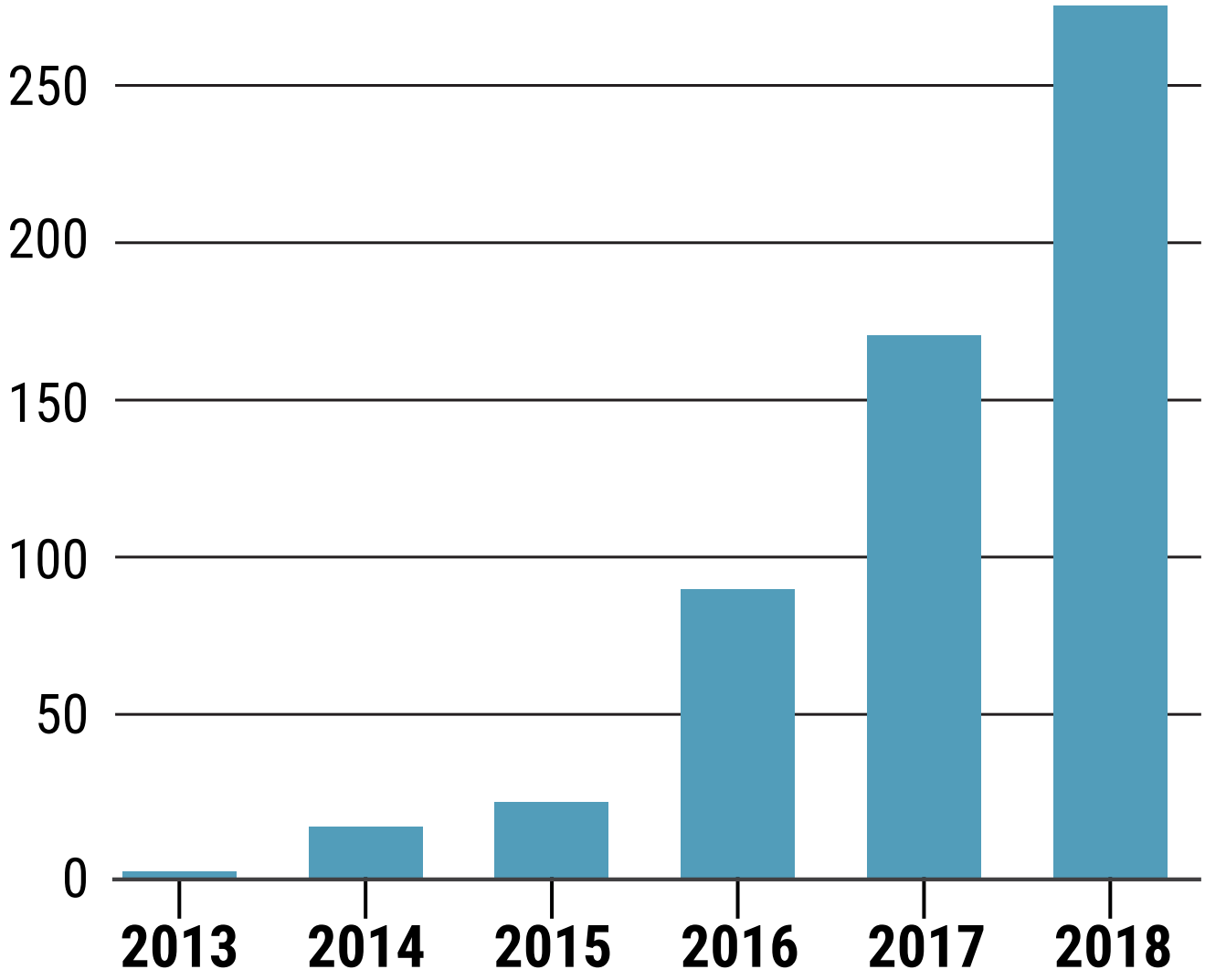

(GRAPHIC) N. DESAI/*SCIENCE*; (DATA) UK BIOBANK

In contrast, the Wellcome Trust and U.K. Medical Research Council insisted that any researcher approved by the UKB board, anywhere in the world, be able to download anonymized data sets on all 500,000 participants. (Users pay a relatively modest fee of $2500 and agree to return their raw data, results, and code to the UKB after publishing. They also sign a legal agreement not to try to reidentify any participant.)

"It was a novel concept," says Collins, who says he's lost track of the times someone has asked him after a talk whether he's interested in collaborating. "I have to say, ‘You just request the data.’ To some extent people don't believe it."

The aim is to maximize the scientific pay-off: "By making data available to 100 people around the world, we can get a lot more research done than if I sit here and do one study a year with the data," he says.

In 2015, his team released the first batch of genetic data on a subset of 150,000 participants. Then came the July 2017 release of full genotyping data for all 500,000. Two months later, Benjamin Neale's group at the Broad Institute put up its blog doubling the number of markers linked to traits and disorders, as well as a web browser for looking up specific markers. "We viewed it as a service to the community," Neale says.

Today, about 7000 researchers have registered to use UKB data on 1400 projects, and nearly 600 papers have been published. Some studies simply link behaviors and disease, for example reporting that drinking more coffee can reduce mortality but that binge-watching TV is associated with more colon cancer. But most studies compare the genomes of people with some trait or disease with those without it, in order to home in on genes that influence that attribute; these projects are known as genome-wide association studies.

The result, every few days, is a new paper using UKB data to link particular gene variants to a disease or trait—arthritis, type 2 diabetes, depression, neuroticism, heart disease. "It's so easy for people who don't collect their own data," says statistical geneticist Danielle Posthuma of Vrije University in Amsterdam, who studies brain diseases. By combining data from the UKB and other collections, investigators can amass samples of a million people or more, amplifying the signal of gene variants with subtle effects. For some diseases, dozens or hundreds of genes appear to play a role. The genetic links are suggestive correlations; establishing cause and effect will take more genetics work and lab studies, which could reveal new disease pathways that might be drug targets.

> **“The U.K. is getting all of the world's best brains [to study its citizens].”**
>
> *Ewan Birney, EMBL European Bioinformatics Institute*

In the near term, the large sample sizes are boosting the power of "polygenic" risk scores, which calculate a person's disease risk by combining many genetic markers. For example, one study published in August 2018 in *Nature Genetics* drew on the July 2017 data to devise risk scores for five diseases, including breast cancer and heart disease. The authors, at Massachusetts General Hospital in Boston and the Broad Institute, found that a surprisingly high 8% of people of European descent have at least a threefold elevated risk for heart disease. And up to 6% have a three-fold increase in risk for one of the four other diseases, suggesting they should be screened early and consider lifestyle changes or other measures that could improve their odds.

The most provocative studies have probed for genetic influences on human behavior. One, published in *Nature Genetics* in July 2018, drew on the UKB and 23andMe to pin down genetic contributions to a person's level of education. Together, 1300 genetic markers accounted for 11% of the variability among individuals, the researchers found. That's comparable to certain environmental influences in the UKB sample, such as family income, which predicted just 7% of the variance in educational attainment among participants; and mother's education level, which predicted 15%. Another study presented at a meeting last fall found four genetic markers that appear to have a **strong influence on whether a person has had sex with someone of their own sex at least once**.

Such studies are raising concerns that genetic tests could be used to screen embryos for desired traits or discriminate against individuals with certain genetic profiles. That would be a misuse of the findings, say the researchers who identified these links. They stress that the probabilities mean little on the individual level.

Long-term investment

Nearly 2 decades after U.K. funding organizations proposed a large, long-term health study, the database is paying off richly; its timeline is punctuated by massive, open-access data releases. Meanwhile, participants age and develop diseases, adding power and momentum to the project.

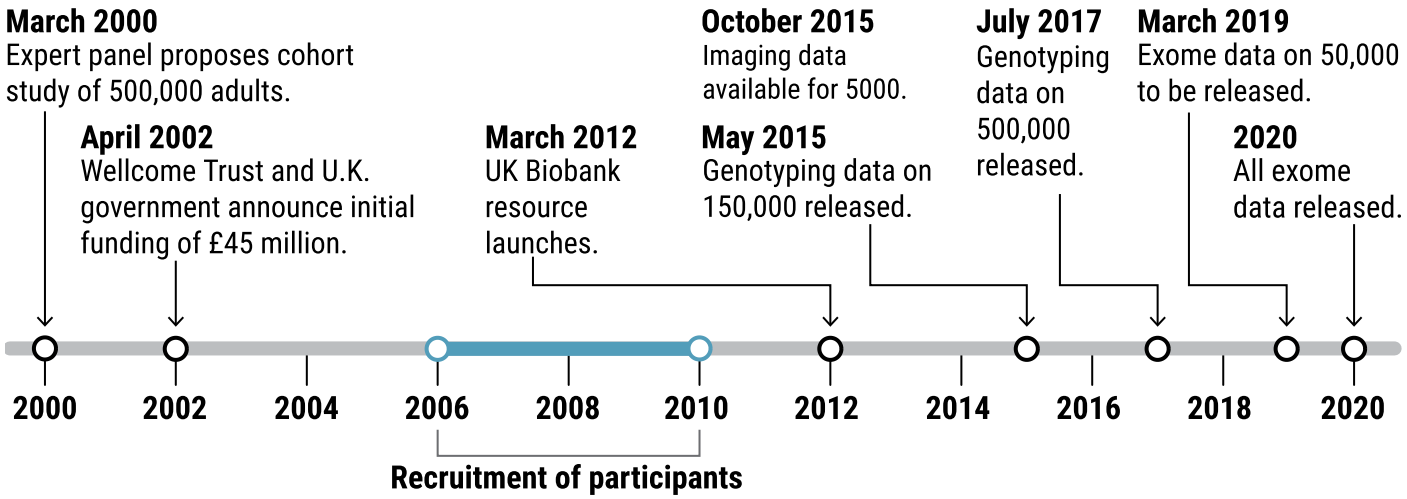

N. DESAI/*SCIENCE*

The UKB's unusual design does have some limitations. The big one: Ninety-four percent of participants are white. "It's really good if you're British or European," Lander says. But, "If you're an American without European ancestry or an African or Asian, you're going to be poorly serviced by the new polygenic risk scores." Nor will scores for traits such as educational attainment be meaningful in people with non-European ancestry.

The mailed invitation recruitment strategy didn't work as well as hoped, says Collins, who notes that young, low-income, white men are also scarce in the database. "We were aiming to get heterogeneity, but it's difficult."

Bishop blames the project's slant toward higher income, healthy, white people on a lack of incentives for participants—they don't get even a small payment or the promise of receiving their test results. The people attracted to the project were those with enough spare time to participate or "who [wanted] to help research," she says.

One problem is that many immigrants to the United Kingdom have little experience with the research world, says Naveed Sattar, an adviser to the UKB and a clinical researcher and epidemiologist at the University of Glasgow. "Most first generation Asians simply have no prior experience of what research is and that it may help their community and their children in the future," he says. Surveys have found that immigrants are often suspicious of participating in research—perhaps because of unethical past studies in some countries, or concern that genetic findings could be used to discriminate.

> **"We were aiming to get heterogeneity, but it's difficult."**
>
> *Rory Collins, UK Biobank principal investigator*

Engaging such groups is possible, says geneticist David Van Heel of Queen Mary University of London, who heads the Genes & Health study, which so far has enrolled 33,000 Britons of Bangladeshi and Pakistani ancestry. In his experience, South Asians in the United Kingdom are less likely to respond to mailed invitations. His project achieved success by approaching potential participants in person—sometimes in their native language—in "trusted" settings such as health clinics and community centers.

Collins and other geneticists hope other biobanks can help fill the gap. For example, the Wellcome Trust is now the main funder of the China Kadoorie Biobank, with data on 515,000 people from mainland China, belonging to 10 ethnic groups. In the United States, the All of Us biobank funded by the National Institutes of Health (NIH) aims to use community outreach to help enroll at least half of its 1 million participants from minority groups, and like the UKB, promises to make data freely available. The Human Heredity & Health in Africa initiative has 70,000 participants so far across the continent, with funding from NIH and the Wellcome Trust. "There are ways of fixing this up. But we've got a long ways to go," Birney says.

Meanwhile, the UKB's riches are growing. About half of the participants' primary care data, including clinical data and prescriptions, will become available next spring. The UKB has also done MRI scans of the brains, hearts, and abdomens of 25,000 participants, with plans to scan 100,000; researchers are examining and annotating the images.

Collins has been promoting the UKB's scientific treasure in Silicon Valley in California, where he hopes bioinformatics experts will dig in and come up with unexpected findings. The genetic data are ballooning, too: Several companies are now sequencing the exomes, or protein-coding regions, of all UKB participants, and the United Kingdom's public Sanger Institute is sequencing whole genomes from 50,000 volunteers. Unlike the genotyping data, which don't usually point to specific genes, the sequences will allow researchers who have found a genetic marker linked to a disease to quickly zero in on the causative gene and see the specific mutations at work.

Because of the $150 million cost of this sequencing work, the UKB had to compromise on open access: Companies have 9 to 12 months to use the exome data before they are made widely available. But Collins and his team, as well as geneticists around the world, are already gearing up for the wide release of the first batch of exome data on 50,000 participants. Again, they'll allow time for the download, then release a code. The starting gun in the next scientific race is set for March.

Posted in: **Biology**, **Health**
doi:10.1126/science.aaw5041

Jocelyn Kaiser

Jocelyn is a staff writer for *Science* magazine.

Email Jocelyn

Ann Gibbons

Ann is a contributing correspondent for *Science*.

Twitter

More from News

Monogamy may have a telltale signature of gene activity

Genetic data on half a million Brits reveal ongoing evolution and Neanderthal legacy

'Nanoscavengers' could protect people from sarin gas, other nerve agents

Got a tip?

How to contact the news team

EXHIBIT F

SCIENCE

Biological Cartographers Seek To Map The Trillions Of Cells In The Human Body

LISTEN · 5:23 QUEUE Download Transcript

January 5, 2019 · 7:56 AM ET
Heard on Weekend Edition Saturday

NELL GREENFIELDBOYCE

There's an effort underway to make a new atlas of all the cells in the human body, and to describe each cell type using all the powerful tools of today's genetic technology.

SCOTT SIMON, HOST:

Your body has around 37 trillion cells - no, really, we've counted, all bodies do, including BJ Leiderman, who writes our theme music - heart cells, liver cells, bone cells. NPR's Nell Greenfieldboyce reports scientists are now using a powerful technology to discover the kinds of cells that weren't

previously recognized, and their goal is to build an atlas of every cell in the human body.

NELL GREENFIELDBOYCE, BYLINE: At the Broad Institute of MIT and Harvard in Boston, I watch a researcher named Julia Waldman consider some bits of what looks like orange Styrofoam. It's skin - frozen, human skin. She selects one of them.

JULIA WALDMAN: I'll put the rest back so we can freeze them and save them for later.

GREENFIELDBOYCE: I don't think I've ever seen frozen skin before. I bet you've...

WALDMAN: (Laughter) Most people haven't.

GREENFIELDBOYCE: I bet you've seen a lot of frozen things.

WALDMAN: I have. I have seen many frozen tissues.

GREENFIELDBOYCE: And fresh tissue samples, too, from human brains, lungs, kidneys, prostates, livers, the gut, fat. They were sent here by clinicians and other researchers because this lab is part of an international effort to look at all these tissues in a radical new way. Waldman kind of crushes the skin in a test tube filled with a chemical solution.

WALDMAN: You can see it's getting cloudy, so the tissue is starting to break up.

GREENFIELDBOYCE: After some more processing to strip away the cell membranes, she's left with nothing but cell nuclei, the control center of each cell. She counts them under a microscope.

WALDMAN: So we have roughly 500,000 nuclei per milliliter, which is great.

GREENFIELDBOYCE: She puts thousands of them into a special device. It encases each cell nucleus in a separate droplet of oil along with a tiny bead of gel that has a unique barcode. When these droplets get run through a machine, the contents of each individual cell nucleus can be analyzed separately, thousands of them all at once.

AVIV REGEV: Whereas before, you know, with very hard work, one person could process a handful.

GREENFIELDBOYCE: Aviv Regev runs this lab. She says, this kind of technology to probe individual cells has only been available in the last few years. She says, every cell in the body basically has the same DNA, the same set of genetic instructions.

REGEV: But every cell reads only a portion of these instructions. And that's why the cells in our liver are different from the cells in our brain and are different from the cells in our skin and so on.

GREENFIELDBOYCE: Now scientists can easily find out what genetic instructions each cell is following, and they can do this on a massive scale. Already, millions of individual cells have been analyzed, and new types of cells have been found in, for example, the lining of the windpipe. Regev and

some of her colleagues plan to catalogue every single cell type in the human body. They call it the Human Cell Atlas.

REGEV: We don't need to analyze every individual cell out of 37 trillion because the cells kind of repeat themselves. All we need to do is sample enough of them from enough region in order to get comprehensive coverage.

GREENFIELDBOYCE: The effort started a couple years ago, and it will take years to complete. But the payoff could be huge with new insights into all kinds of diseases. Sarah Teichmann is head of cellular genetics at the Wellcome Trust Sanger Institute in Cambridge, England. She's one of the leaders of the Human Cell Atlas, and she and her colleagues recently took a close look at kidney cancer. They analyzed 72,000 cells from healthy and cancerous human kidneys.

SARAH TEICHMANN: And so that was really exciting, both in terms of the basic understanding of the kidney cells but also for the cancer community in terms of understanding where these tumor cells come from.

GREENFIELDBOYCE: A child who had kidney cancer, for example, seemed to come from aberrant fetal cells while some adult cancers came from a different, little-studied subset of cells.

TEICHMANN: I mean, the methods are just so powerful. It really is mind-boggling, incredibly exciting and, you know, I need to pinch myself sometimes.

GREENFIELDBOYCE: She says the human body contains more than 50 different tissues. Some get a lot of attention, like the brain. Others are kind of ignored.

TEICHMANN: There are some that you probably haven't even heard of, you know, funny stuff like omentum.

GREENFIELDBOYCE: That's a sheet of fatty tissue that wraps around the intestines. The Human Cell Atlas wants to get everything from that to the inner ear. The whole plan staggers folks who study cells and tissues in more traditional ways, like with microscopes and stained slides. Rosy Jurjus is an associate professor of anatomy and cell biology at George Washington University. She recently attended a workshop for folks who are mapping the human body at the cellular level.

ROSY JURJUS: And I remember actually being very excited all through the workshop because it's groundbreaking. It's new, and it's the future.

GREENFIELDBOYCE: Meanwhile, researchers have been building complete cell atlases of creatures that are commonly studied in the lab to give insights on human biology. They've already finished one for a famous laboratory worm, C. elegans. Unlike humans, it has hundreds rather than trillions of cells. Nell Greenfieldboyce, NPR News.

EXHIBIT G

Progress Towards a Systematic Comparison of Single Cell RNA-Seq Methods

Jiarui Ding[1], Xian Adiconis[1], Sean K. Simmons[1], Cynthia C. Hession[1], Nemanja D. Marjanovic[1], Monika Kowalczyk[1], Travis K. Hughes[1-4], Marc H. Wadsworth[1-4], Tyler Burks[1], Mandovi Chatterjee[5], Lan Nguyen[1], Danielle Dionne[1], John Y. H. Kwon[1], Shaina Carroll[2-4], Alex Ratner[5], Shuqiang Li[1], Sarah A. Boswell[5], Nir Hacohen[1,6], Orit Rozenblatt-Rosen[1], Alex K. Shalek[1-4], Alexandra-Chloé Villani[1,7], Aviv Regev[1,4,8], **Joshua Z. Levin**[1]

[1]Broad Institute of MIT & Harvard, Cambridge, MA USA [2]Institute for Medical Engineering & Science, Dept. of Chemistry, MIT, Cambridge, MA USA
[3]Ragon Institute of MGH, MIT, and Harvard, Cambridge, MA USA [4]Koch Institute of Integrative Cancer Research, Cambridge, MA USA [5]Single Cell Core, Harvard Medical School, Boston, MA USA
[6]Center for Cancer Research, Dept. of Medicine, Massachusetts General Hospital, Boston, MA USA [7]Center for Immunology and Inflammatory Diseases, Massachusetts General Hospital, Charlestown, MA USA
[8]Howard Hughes Medical Institute, Dept. of Biology, MIT, Cambridge, MA USA

Summary

Statement of Purpose: We are directly comparing single cell RNA-Seq methods to understand their relative advantages and disadvantages.

Background
- Single-cell RNA sequencing (scRNA-Seq) has emerged as a powerful tool to understand many areas of biology.
- For Human Cell Atlas (HCA) and many other single cell transcriptomic projects, there is a critical need to assess which scRNA-Seq methods are best for particular applications.
- An updated comparison of methods is needed.

Methods
- Plate-based: Smart-seq2, CEL-Seq2
- Bead-based: 10x Chromium, Drop-Seq, Seq-Well, inDrops
- "*In situ*": sci-RNA-seq

Experimental Design

Mixing
- Grew NIH3T3 (mouse) and HEK293 (human) cell lines
- Prepared aliquots as cell suspensions (mixtures with 50% of each cell line) in appropriate buffers for each method

PBMCs
- Thawed human Peripheral Blood Mononuclear Cells (PBMCs)
- Prepared aliquots as cell suspensions in RPMI + 2% human serum, resuspended in buffers for each method

- Prepared all libraries in parallel — starting processing at same time.
- Aimed for 384 cells (plate-based), ~3000–4000 cells (bead-based), ~7,500 cells (*in situ*)
- Sequenced all libraries usually pooled together (minimize batch effects), except inDrops because of read structure.
- Performed two replicates for each sample type

Computational Analysis

- Created universal pipeline for data from all methods.
- De-multiplexed CEL files, allowing one error per index.
- Aligned reads to combined human hg19 & mouse mm10 genomes (mixing) or GRCh38 (PBMCs) using HISAT2 (Smart-seq2, CEL-Seq2) or STAR (others).
- Generated cell-gene UMI/read matrices from aligned reads; and cell-gene expression matrices (grouped UMIs based on Hamming distance of one).
- **Mixing**: Selected candidate cell barcodes with ≥10% of expected library size for bead based and 'In situ' methods.
- **Mixing**: Modeled number of reads per cell as a mixture distribution & removed cell barcodes with fewer reads.
- **PMBC**: Selected 2x expected # cell barcodes, cluster, remove cells in "low quality" clusters. Permits recovery of cell types with low RNA content.

Single Cell RNA-Seq Methods

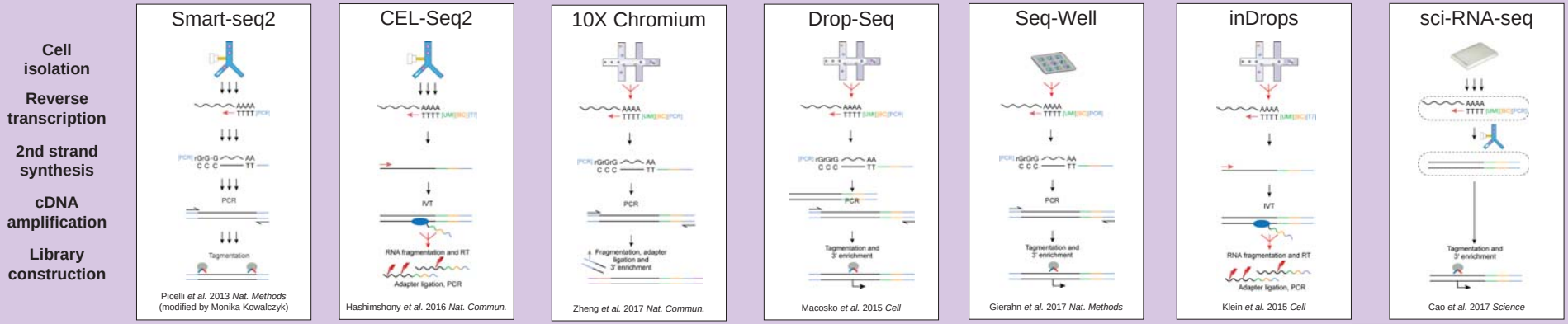

Picelli *et al.* 2013 *Nat. Methods* (modified by Monika Kowalczyk)
Hashimshony *et al.* 2016 *Nat. Commun.*
Zheng *et al.* 2017 *Nat. Commun.*
Macosko *et al.* 2015 *Cell*
Gierahn *et al.* 2017 *Nat. Methods*
Klein *et al.* 2015 *Cell*
Cao *et al.* 2017 *Science*

Adapted from Ziegenhain *et al.* 2017 *Molecular Cell*

Results

Basic Metrics (Mixing #2)

Metric/Method	Smart-seq2	CEL-Seq2	10X Chromium	Drop-Seq	Seq-Well (v1)	Seq-Well (v2)	inDrops	sci-RNA-seq
Total reads	327M	361M	354M	287M	287M	111M	133M	459M
# cells (expected)	376	383	4,000	3,500	2,500	2,500	4,000	7,680
# cells (detected)	343	347	3,187	3,812	1,012	837	2,529	5,023
Total reads / cell (detected)	952,738	1,039,165	111,149	75,326	283,795	133,108	52,727	91,385
Doublets (detected)	0.0%	0.6%	1.2%	3.5%	3.2%	3.1%	3.4%	3.1%

Basic Metrics (PBMC #2)

Metric/Method	Smart-seq2	CEL-Seq2	10X Chromium	Drop-Seq	Seq-Well (v1)	Seq-Well (v2)	inDrops
Total reads	250M	278M	319M	704M	236M	606M	503M
# cells (expected)	376	383	4,000	3,500	5,000	5,000	5,000
# cells (detected)	309	303	3,362	6,412	5,125	5,640	7,053
Total reads / cell (detected)	775,555	917,666	95,003	109,769	45,972	107,382	71,288

Note: sci-RNA-seq was unsuccessful for PBMCs in 4 attempts.

How many cells did we detect?
- Not possible to predict well how many cells will be detected.
- Choosing more cells lowers the median # genes/cell.
- One solution is to plot genes/cell vs. cells ranked from most to least genes/cell.

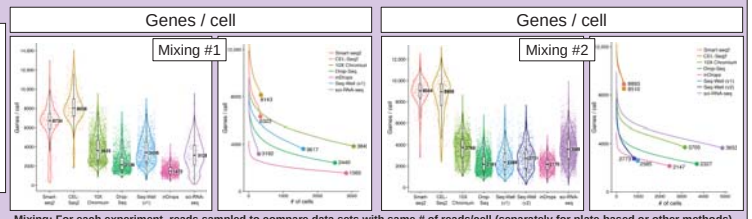

Mixing: For each experiment, reads sampled to compare data sets with same # of reads/cell (separately for plate-based or other methods).

Cluster scoring
- Louvain algorithm used to partition undirected KNN graphs into non-overlapping clusters
- Each cell assigned cell-type scores using known marker genes
- Area Under Curves (AUCs) calculated from cell-type scores used to assign cell types to clusters

PBMC analysis preliminary – not downsampled

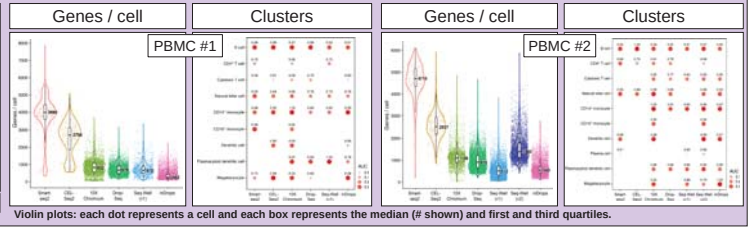

Violin plots: each dot represents a cell and each box represents the median (# shown) and first and third quartiles.

Future Directions

- Finish down-sampling (reads & cells) for firmer conclusions
- Compare to standard computational pipelines
- Compare single nucleus methods (with mouse cortex): Smart-seq2,10X Chromium, DroNc-Seq & sci-RNA-seq (*analysis in progress*)
- Evaluate ability to identify cell sub-types: CD8 T cells (*analysis in progress*)
- Assess value of Smart-seq2 full length data in combination with 3' end transcriptome data

Acknowledgements

We thank Leslie Gaffney for help with figures, the Broad Genomics Platform for sequencing, the Broad Flow Cytometry Facility for FACS, Michael Cuoco for sample transport, Allon Klein for advice, and Jane Lee and Anna Neumann for project management.

EXHIBIT H

Angewandte Chemie

Communications

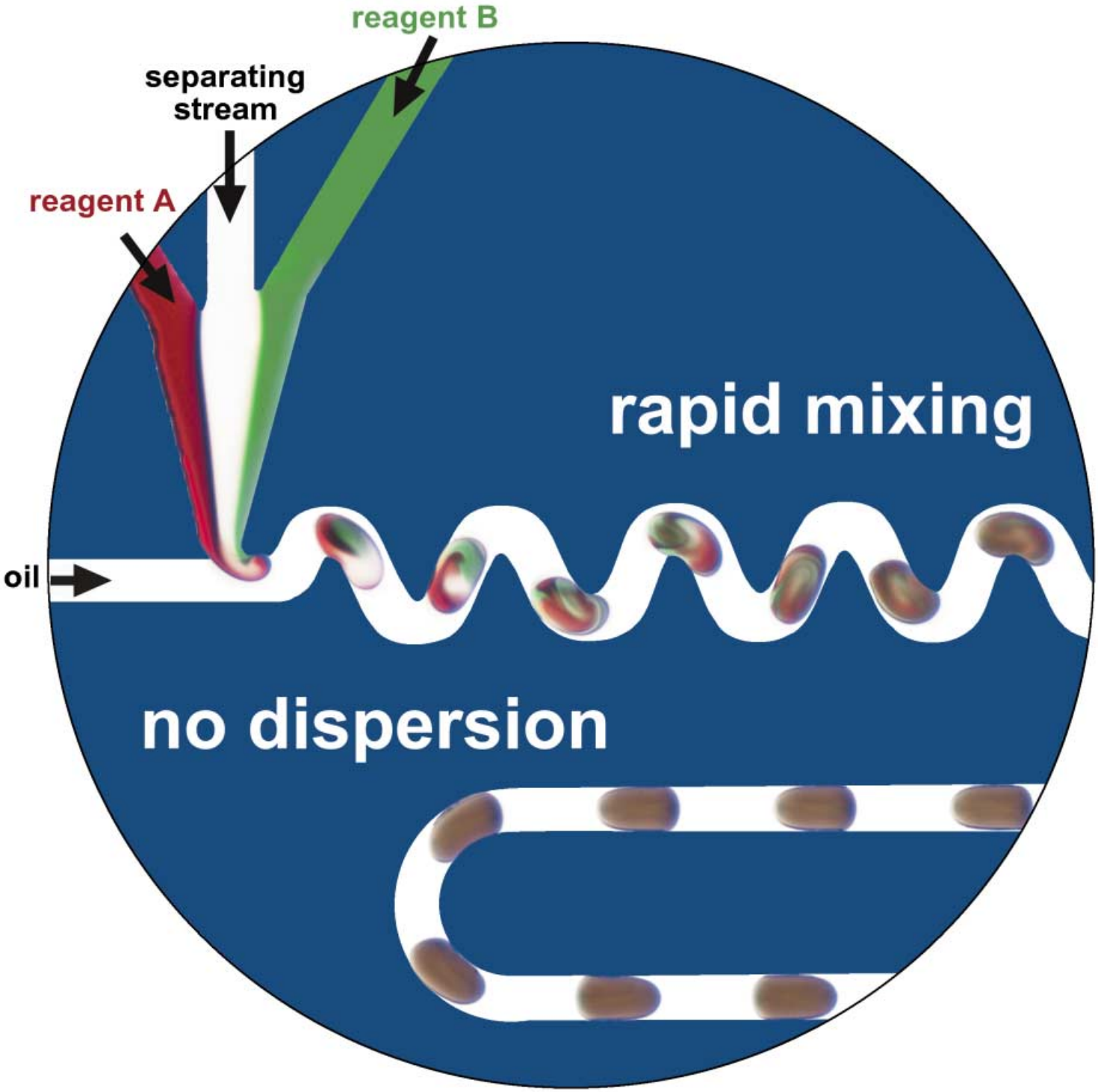

Aqueous droplets of 250 pL formed in a microfluidic channel in a continuous flow of a water-immiscible fluid act as microreactors that mix the reagents rapidly and transport them with no dispersion. These droplets may also be used to control chemical reaction networks on millisecond time scale. For more information see the following publication by R. F. Ismagilov et al.

  1433-7851/03/4207-0767 $ 20.00+.50/0

High-Throughput Measurements

A Microfluidic System for Controlling Reaction Networks in Time**

*Helen Song, Joshua D. Tice, and Rustem F. Ismagilov**

We present here a microfluidic system that may be used to control networks of many chemical reactions on the millisecond scale. It allows to control when each reaction begins, for how long each reaction evolves before it is separated or combined with other reactions, and when each reaction is analyzed or quenched. The system uses flow of fluids to linearly transform space (length of capillaries) into time (reaction time). For a chemical reaction in an open system this transformation is simple and well known: A solution of reagent A and a solution of reagent B are injected as steady streams into a microfluidic channel at initial point $d = 0$ where the reaction between them begins ($t = 0$). As the reaction mixture is transported by the fluid stream at a constant velocity U, every spatial point d corresponds to a time point t, the reaction time, where $t = d/U$. If such a system is implemented, interactions of multiple chemical reactions in time could be controlled simply by creating a network of converging and diverging channels carrying reaction mixtures, and varying flow velocities to adjust reaction and interaction times. If the reactions are accompanied by an optical signal (e.g. changes in fluorescence or absorption), time-resolved measurements of the reactions in the entire network could be obtained from a single spatially resolved optical image.

Networks of microfluidic channels[1–3] are especially attractive for this distance-to-time transformation because they can be easily fabricated and used to manipulate small volumes of reagents; they are becoming essential for chemical and biological analysis and synthesis.[1–3] Flow in microfluidic devices is laminar; it occurs at low values of the Reynolds number, Re (~0.01–100). Re is defined as $lU\rho/\mu$, where l [m] is the diameter of the capillary, U [m s^{-1}] the velocity of the flow, ρ [kg m^{-3}] the density, and μ [kg m^{-1} s^{-1}] the viscosity of the fluid.[4] This laminar flow makes it difficult to implement the distance-to-time transformation in microfluidic devices for two reasons (Figure 1a). First, mixing is slow—two streams injected into a channel flow side-by-side with mixing only by diffusion,[4–6] therefore $d = 0$ does not correspond to a well-defined starting point ($t = 0$) of the reaction. Significant research efforts have been devoted to solving this problem of slow mixing.[2,3,7] Turbulent flows provide both rapid mixing and low dispersion,[8] but turbulence occurs at values of $Re > 2000$ reached in microchannels only at high flow rates (~10 m s^{-1}). Achieving such flow velocities requires undesirably high sample consumption (~1 mL s^{-1}) and high pressures. Second, the dispersion of solutes along the channel is large—the flow profile is parabolic, and the reagents are transported at a range of velocities.[4] Therefore, a given distance d corresponds to a range of reaction times $t = d/U$.

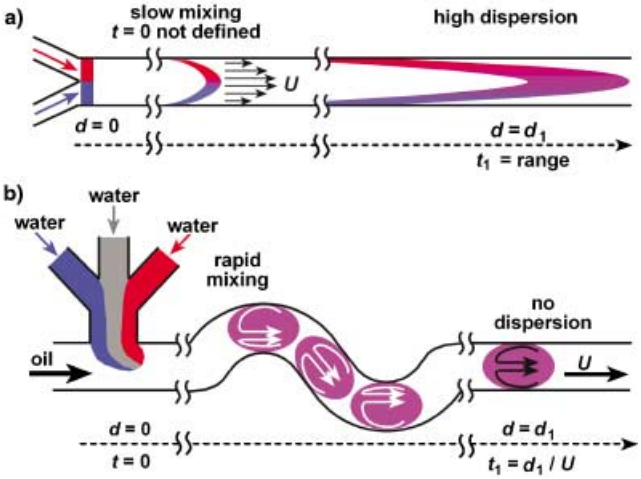

Figure 1. Schematic comparison of a reaction A + B conducted in a standard pressure-driven microfluidic system device (a) and in the microfluidic device described here (b). a) Reaction time $t \neq d/U$. b) Reaction time $t = d/U$. Two aqueous reagents (red, A and blue, B) can form laminar streams separated by a gray "divider" aqueous stream in a microchannel. When the three streams enter the channel with a flowing immiscible fluid, they form droplets (plugs). The reagents come into contact as the contents of the droplets are rapidly mixed. Internal recirculation within plugs flowing through channels of different geometries is shown schematically by arrows.

We developed a simple microfluidic system that overcomes both problems—it transports solutions with rapid mixing and no dispersion (Figure 1b). This system uses networks of microchannels with rectangular cross sections and hydrophobic surfaces fabricated using rapid prototyping in polydimethylsiloxane (PDMS).[9] We controlled the volumetric flow rates through each channel using syringe pumps. Dispersion was eliminated by localizing the reagents within aqueous plugs (droplets large enough to block the channel) separated by a water-immiscible oil. Immiscible fluids have been used to localize reagents in both commercial[10] and laboratory[11–13] systems. Here we describe methods for forming plugs of multiple solutions of reagents, for using chaotic advection to achieve especially rapid (~2 ms) mixing within the plugs, and for splitting and merging these plugs in order to create complex microfluidic networks.

To form droplets from two solutions of reagents without bringing the reagents into prior contact we flowed these

[*] Prof. R. F. Ismagilov, H. Song, J. D. Tice
Department of Chemistry
The University of Chicago
5735 S. Ellis Avenue, Chicago, IL 60637 (USA)
Fax: (+1) 773-702-0805
E-mail: r-ismagilov@uchicago.edu

[**] This work was supported by the Camille and Henry Dreyfus New Faculty Award Program, the Searle Scholars Program, an award from Research Corporation, the Chicago MRSEC funded by the NSF. H.S. was supported by a Predoctoral Training Grant of the NIH (GM08720). We thank our colleagues at the University of Chicago for invaluable discussions and suggestions. We thank Prof. Sidney Nagel, in addition, for an equipment loan and Ian Hawkins for measuring surface tensions. Photolithography was performed by H.S. at MAL of the University of Illinois at Chicago. Microscopy was conducted at the University of Chicago Cancer Center Digital Light Microscopy Facility.

  1433-7851/03/4207-0768 $ 20.00+.50/0

solutions in a microchannel as two laminar streams,[14] and used an inert center stream to separate them. These three streams were continuously injected into a flow of water-immiscible perfluorodecaline (PFD) in the main microchannel, where they spontaneously broke up into streams of plugs (~500 pL) separated and surrounded by PFD (Figure 2). Diffusion through the central stream was too slow for the reagents in the two side streams to interact prior to the formation of a plug. Plugs of three or more reagents could be formed in the same manner. PFD is an attractive choice of carrier fluid because it is inert, immiscible with water and organic solvents, and does not swell PDMS. Emulsions of perfluorocarbons such as PFD are used as blood substitutes in humans during surgeries[15] and should be compatible with a range of biological molecules. We controlled the wetting of PDMS by PFD by adding 9% v/v of $C_6F_{11}C_2H_4OH$ to PFD. Water-in-oil emulsions are known to form in pressure-driven flow in microchannels,[16,17] often at high values of the dimensionless capillary number, Ca ($Ca = U\mu/\gamma$, γ [$N\,m^{-1}$]: surface tension at the PFD/water interface).[18] Our system was operated at low values of Ca because at high values of Ca, the shear flow broke up the aqueous phase into small droplets that did not block the channels and were not transported reliably over long distances. Complex behavior in this latter regime has been carefully characterized.[16]

A plug moving in a straight channel generates a steady, recirculating flow.[19] This flow mixes the fluid within the left and the right (along the direction of the flow) halves of the plug (black arrows in Figure 1b, right), but not between the two halves. Laminar flow is preserved during plug formation that occurs at low Re; the reagent solutions end up in the two halves of the plug, and internal recirculation within elongated plugs enhances mixing only moderately (Figure 2).

Chaotic advection accelerates mixing by using unsteady fluid flow to stretch and fold a volume of fluid. Stretching and folding leads to a rapid, exponential decrease of the striation length—distance over which mixing has to occur by diffusion. At intermediate Re ($Re \sim 70$), chaotic advection can be generated in three-dimensional microfluidic systems.[20] An elegant system used asymmetric ridges on the floor of a microchannel to induce chaotic advection at both low and intermediate values of Re ($Re = 0$–100).[7] Here we show how the principles of chaotic advection can be applied to mixing inside plugs.

The principle of chaotic advection has been illustrated with flow-cavity experiments.[21] In a flow cavity, motion of the top and bottom walls induces flow within a volume of fluid. Simultaneous motion of these walls induces steady flow that mixes solutions slowly (Figure 3a). Time-periodic, alternating motion of the walls induces unsteady, chaotic flow that mixes solutions rapidly (Figure 3b). Crossing of streamlines in this time-periodic flow is a necessary condition for chaos.[21]

Fluid flow in a flow cavity is similar to fluid flow in a plug moving inside a channel, except for the frame of reference—in a flow cavity walls move relative to the fluid, and in a plug fluid moves relative to the walls. Steady flow in a flow cavity is similar to steady, recirculating flow in plugs moving in a straight channel (black arrows in Figure 1b right). For arbitrary initial conditions, mixing by this steady flow is inefficient (efficiency decreases as $1/t$)[19,21] because solutes become trapped on the streamlines that do not cross.[21] For example, this flow mixes the contents within the left and right halves of the plug, but not between the two halves (Figure 2). The two-dimensional component of this flow responsible for mixing of the solutions can be envisioned as two counter-rotating vortices located in the left and right halves of the plug (white arrows in Figure 1b). In the flow cavity shown in Figure 3 the two vortices are co-rotating.

Pairs of co-[22–24] and counter-rotating[24,25] vortices both generate chaos in periodic time-dependent flow. We induced such a flow in plugs by replacing a straight channel with a winding channel (Figure 4). A plug moving through a curved part of the winding channel is moving at different velocities relative to the two walls, similar to fluid in a flow cavity of Figure 3b. We have deduced the streamlines shown by the

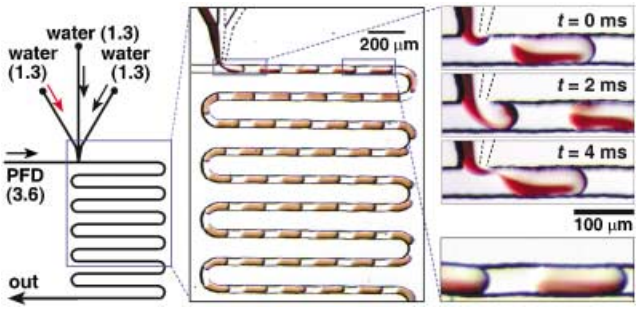

Figure 2. Spontaneous formation of uniform plugs out of multiple aqueous streams. Left: Schematic diagram of the microchannel network. Volumetric flow rates for all streams (in $\mu L\,min^{-1}$) are given in parenthesis. Middle: Microphotograph (10 μs exposure) of plug formation and transport. Right: Magnified microphotographs (10 μs exposure) of the plug-forming region at different time points. All microchannels had $50 \times 50\ \mu m^2$ cross sections. Total flow rate in the main channel: $7.5\ \mu L\,min^{-1}$ ($50\ mm\,s^{-1}$ average flow velocity); $Re \sim 2.5$ (water), ~0.93 (PFD). PFD here stands for a 10:1 mixture of perfluorodecaline and $C_6F_{11}C_2H_4OH$. Red stream: solution of $[Fe(SCN)_x]^{(3-x)+}$ prepared by mixing 0.067 M $Fe(NO_3)_3$ with 0.2 M KSCN; colorless streams: 0.2 M KNO_3.

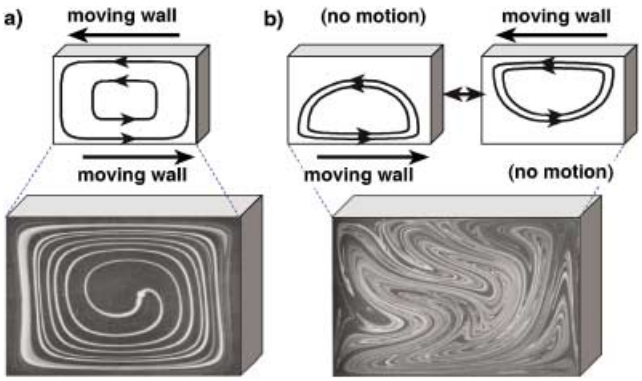

Figure 3. Mixing by steady (a) and time-periodic (b) flows in flow cavities. a, b) Top: Schematic illustration of the flow cavity. The vertical walls are stationary and the horizontal walls move as shown. Bottom: Images (reprinted with permission of Cambridge University Press from ref. [21]) that illustrate the flow patterns. For details, see text.

  1433-7851/03/4207-0769 $ 20.00+.50/0

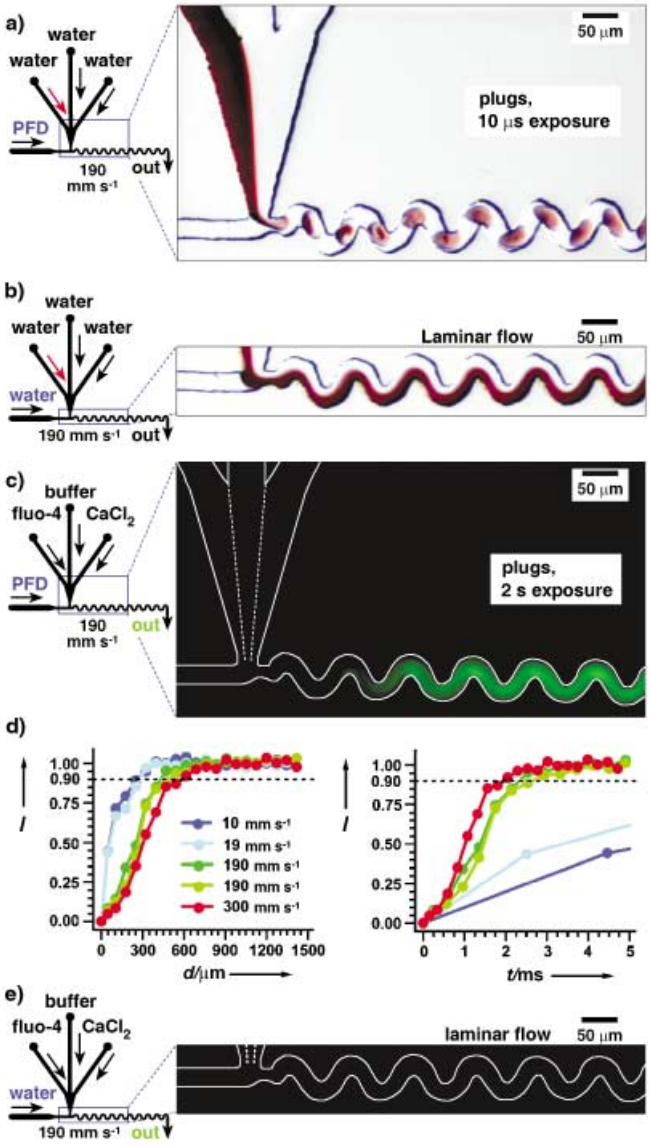

Figure 4. a), b) Microphotographs (10 μs exposure) illustrating rapid mixing inside plugs (a) and negligible mixing in a laminar flow (b) moving through winding channels at the same total flow velocity; same solutions as for Figure 2. c) A false-color microphotograph (2 s exposure, individual plugs are invisible) showing time-averaged fluorescence arising from rapid mixing inside plugs of solutions of Fluo-4 (54 μM) and $CaCl_2$ (70 μM) in aqueous sodium morpholine propanesulfonate buffer (20 mM, pH 7.2); this buffer was also used as the middle aqueous stream. d) Relative normalized intensity (I) of fluorescence obtained from images such as shown in (c) as a function of distance (left) traveled by the plugs and of time required to travel that distance (right) at a given flow rate. The total intensity across the width of the channel was measured. Total PFD/water volumetric flow rates (in $\mu L\,min^{-1}$) were ● 0.6:0.3, ● 1.0:0.6, ● 12.3:3.7, ● 10:6, ● 20:6. e) A false-color microphotograph (2 s exposure) of the weak fluorescence arising from negligible mixing in a laminar flow of the solutions used in (c). All channels were 45 μm deep; inlet channels were 50 μm and winding channels 28 μm wide; $Re \sim 5.3$ (water), ~ 2.0 (PFD).

white arrows in Figure 1b by observing asymmetric plugs traveling through curved channels; these streamlines are similar to those shown in Figure 3b. In plugs moving through winding channels we observed flow patterns that corresponded to very rapid mixing (Figure 4a). These flow patterns were reproducible, and were similar for plugs moving at different speeds, except for some blurring by diffusion at lower speeds. At these low values of Re, winding channels did not accelerate mixing in laminar flow in the absence of PFD (Figure 4b).

In Figure 4c,d we show that this system can be used to measure the rates of chemical reactions on the millisecond time scale, and that these rates can be used to quantify mixing.[6] This was done by measuring the rate of rapid binding ($k_{on} = 7.1 \times 10^8\,M^{-1}\,s^{-1}$)[26] of Ca^{2+} ions to the calcium-sensitive dye fluo-4 (Figure 4c). Fluo-4 is weakly fluorescent in the absence of calcium whereas the complex fluo-4·Ca^{2+} shows strong fluorescence; accordingly, increase in fluorescence corresponds to mixing. At every flow rate we obtained a complete time-resolved reaction profile by acquiring a single spatially resolved long-exposure image of the fluorescence.[8] Each image was integrated over two seconds to give the average fluorescence intensity of hundreds of moving plugs (~60 pL in volume) and non-fluorescent PFD, and consumed less than 50 nL of fluo-4 solution. For the laminar flow of these solutions in the absence of PFD only weak fluorescence was observed (Figure 4e) consistent with negligible mixing shown in Figure 4b. Mixing of $CaCl_2$ and fluo-4 solutions in the plugs was achieved within a short distance (~500 μm, Figure 4d), which was not very sensitive to the PFD/water ratio, and was weakly dependent on flow velocity. At higher flow rates it corresponded to mixing in about 2 ms (Figure 4d).

These facts and the flow patterns in Figure 4a are consistent with chaotic mixing, but detailed modeling would be required to identify the chaotic regions within the plugs. Such modeling would have to account for the three-dimensional recirculation within both aqueous plugs and PFD in a given geometry and should suggest the geometry of the winding channels—symmetric or asymmetric, regular or random—required for most efficient mixing.

A key attractive feature of microfluidics is the possibility of creating large fluidic networks.[27] To demonstrate how, in principle, a network with complex connectivity could be created with this system we designed methods for combining two streams of plugs into a single stream in a main channel (merging plugs), and for dividing one stream of plugs into two streams (splitting plugs). Merging was rare when the main channel was of the same width as the channels in which the plugs formed as plugs merged only if they entered the main channel simultaneously (in phase). Plugs that entered out of phase continued through the main channel separated by PFD because they all moved at the same constant velocity. By contrast, merging was achieved in a wide main channel, even for streams of plugs that were out of phase (Figure 5a). We formed small and large plugs in 30-μm and 60-μm wide channels, respectively. These plugs did not block the expanded 100-μm wide main channel and could move at two different velocities until they coalesced.[28] Small droplets moved more slowly than large droplets;[16] this effect is well known and is the basis of hydrodynamic chromatography.[29] Sufficiently large fluctuations in the relative flow rates in the two channels disrupted merging, but more than 95% of the plugs merged

  1433-7851/03/4207-0770 $ 20.00+.50/0

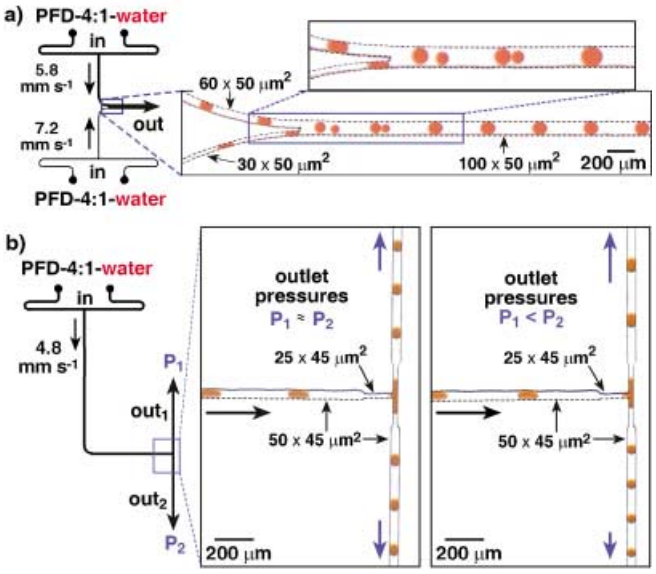

Figure 5. a) Spontaneous merging of pairs of plugs into single plugs. Left: schematic diagram of the microfluidic network; right: microphotograph of two streams of plugs merging in a main microchannel. b) Spontaneous splitting of plugs at a branching point in a microchannel. Left: schematic diagram of the microchannel network and the experimental conditions used. Middle: microphotograph showing splitting of a stream of plugs into plugs of approximately one-half the volume of the initial plugs. The outlet pressures were equal for the two channels. Right: asymmetric splitting of both aqueous and PFD plugs occurred when hydrostatic pressure of about 6 kPa was applied to the second outlet. a), b) Volumetric PFD/water flow rate ratios, flow velocities, and cross-sectional dimensions of the channels (width × height) are also shown.

correctly when flows were simply driven with pressure of compressed air from a house line, regulated manually.

Reliable splitting of plugs at branching points of microchannels was achieved by constricting the channels at the branching points. When the channels were not constricted, short rounded plugs often showed a complicated behavior dominated by the surface tension at the PFD/water interfaces. In constricted channels the plugs became long and narrow and behaved simply like laminar flows subjected to pressure gradients (Figure 5b). The size of the split plugs was proportional to the relative flow rates in the two outlet channels; we controlled these flow rates by varying the relative hydrostatic pressures at the two outlets. Splitting and subsequent merging of plugs could become useful for high-throughput parallel measurements. These methods of merging and splitting rely on a simple control of widths of channels and should become especially useful in combination with advanced methods of pumping.[30]

Overall, the phenomena described here allow us to construct a microfluidic system that linearly converts distance into time by achieving millisecond mixing and transport with no dispersion. We believe that it will be useful for both chemical analysis and synthesis, and for studies of complex reaction networks.[31] The system is easy to fabricate and operate, has no active or moving components, and can be controlled simply by varying the rates of fluid flow. The uncertainty of the distance-to-time transformation is limited by the mixing distance. Both short (ms) and long (min) time scales can be accessed in the same microfluidic device simply by varying the flow velocity. Sub-millisecond time scales should be accessible by decreasing the size of the channels, and by increasing the flow rate (as long as the capillary number remains small). In a serpentine microfluidic network an entire time course of a chemical reaction can be obtained with millisecond resolution by analyzing fluorescence from a single image. Because the flows are steady this image does not have to be time-resolved[8] and can be obtained with long exposures of a CCD or even a photographic camera. This system consumes samples at a rate about 10000 times lower ($\mu L\,min^{-1}$) than devices that rely on turbulence for mixing ($mL\,s^{-1}$). It may serve a broad community of chemists, biochemists, and biophysicists as an inexpensive compliment to stop-flow instruments. In addition to a planar, trivial to fabricate, disposable plastic chip it only requires equipment already present in most laboratories: a source of pressure, such as a syringe pump or a cylinder of compressed gas, and a microscope with a CCD camera. We believe that this system for conducting reactions in sub-nanoliter plugs will also become valuable in traditional areas of microfluidics where miniaturization and speed are important—for example, high-throughput screening, combinatorial synthesis, analysis, and diagnostics—both as a self-contained platform, and in combination with the existing technologies, especially those using flows of immiscible fluids.[32,33]

Received: September 6, 2002 [Z50110]

[1] M. A. Burns, *Science* **2002**, *296*, 1818.
[2] P.-A. Auroux, D. Iossifidis, D. R. Reyes, A. Manz, *Anal. Chem.* **2002**, *74*, 2623.
[3] P.-A. Auroux, D. Iossifidis, D. R. Reyes, A. Manz, *Anal. Chem.* **2002**, *74*, 2637.
[4] R. B. Bird, W. E. Stewart, E. N. Lightfoot, *Transport Phenomena*, Wiley, New York, **2002**.
[5] A. E. Kamholz, P. Yager, *Sens. Actuators B* **2002**, *82*, 117.
[6] R. F. Ismagilov, A. D. Stroock, P. J. A. Kenis, G. Whitesides, H. A. Stone, *Appl. Phys. Lett.* **2000**, *76*, 2376.
[7] A. D. Stroock, S. K. W. Dertinger, A. Ajdari, I. Mezic, H. A. Stone, G. M. Whitesides, *Science* **2002**, *295*, 647.
[8] M. C. R. Shastry, S. D. Luck, H. Roder, *Biophys. J.* **1998**, *74*, 2714.
[9] J. C. McDonald, D. C. Duffy, J. R. Anderson, D. T. Chiu, H. K. Wu, O. J. A. Schueller, G. M. Whitesides, *Electrophoresis* **2000**, *21*, 27.
[10] D. D. Cunningham, *Anal. Chim. Acta* **2001**, *429*, 1.
[11] M. A. Burns, B. N. Johnson, S. N. Brahmasandra, K. Handique, J. R. Webster, M. Krishnan, T. Sammarco, P. M. Man, D. Jones, D. Heldsinger, C. H. Mastrangelo, D. T. Burke, *Science* **1998**, *282*, 484.
[12] K. Handique, D. T. Burke, C. H. Mastrangelo, M. A. Burns, *Anal. Chem.* **2001**, *73*, 1831.
[13] K. Hosokawa, T. Fujii, I. Endo, *Anal. Chem.* **1999**, *71*, 4781.
[14] P. J. A. Kenis, R. F. Ismagilov, G. M. Whitesides, *Science* **1999**, *285*, 83.
[15] J. E. Squires, *Science* **2002**, *295*, 1002.
[16] T. Thorsen, R. W. Roberts, F. H. Arnold, S. R. Quake, *Phys. Rev. Lett.* **2001**, *86*, 4163.
[17] S. Sugiura, M. Nakajima, M. Seki, *Langmuir* **2002**, *18*, 5708.

  1433-7851/03/4207-0771 $ 20.00+.50/0

[18] The viscosity of PFD is 5.10×10^{-3} kg m^{-3} s^{-1}, the surface tension at the interface between water and fluorinated phase was 13×10^{-3} N m^{-1}. We have shown that this system can be operated at values of *Ca* up to about 0.1 (at 300 mm s^{-1}). As the value of *Ca* increases above about 0.2, the formation of plugs becomes irregular.
[19] K. Handique, M. A. Burns, *J. Micromech. Microeng.* **2001**, *11*, 548.
[20] R. H. Liu, M. A. Stremler, K. V. Sharp, M. G. Olsen, J. G. Santiago, R. J. Adrian, H. Aref, D. J. Beebe, *J. Microelectromech. Syst.* **2000**, *9*, 190.
[21] J. M. Ottino, *The Kinematics of Mixing: Stretching, Chaos, and Transport*, Cambridge University Press, Cambridge, **1989**.
[22] H. Aref, *J. Fluid Mech.* **1984**, *143*, 1.
[23] W. L. Chien, H. Rising, J. M. Ottino, *J. Fluid Mech.* **1986**, *170*, 355.
[24] S. C. Jana, G. Metcalfe, J. M. Ottino, *J. Fluid Mech.* **1994**, *269*, 199.
[25] T. H. Solomon, J. P. Gollub, *Phys. Rev. A* **1988**, *38*, 6280.
[26] M. Naraghi, *Cell Calcium* **1997**, *22*, 255.
[27] T. Thorsen, S. J. Maerkl, S. R. Quake, *Science* **2002**, *298*, 580.
[28] J. Eggers, J. R. Lister, H. A. Stone, *J. Fluid Mech.* **1999**, *401*, 293.
[29] H. Small, M. A. Langhorst, *Anal. Chem.* **1982**, *54*, A892.
[30] M. A. Unger, H. P. Chou, T. Thorsen, A. Scherer, S. R. Quake, *Science* **2000**, *288*, 113.
[31] A. Arkin, P. D. Shen, J. Ross, *Science* **1997**, *277*, 1275.
[32] B. Zhao, N. O. L. Viernes, J. S. Moore, D. J. Beebe, *J. Am. Chem. Soc.* **2002**, *124*, 5284.
[33] M. Tokeshi, T. Minagawa, K. Uchiyama, A. Hibara, K. Sato, H. Hisamoto, T. Kitamori, *Anal. Chem.* **2002**, *74*, 1565.

  1433-7851/03/4207-0772 $ 20.00+.50/0

EXHIBIT I

Langmuir **2003,** *19,* 9127−9133

Formation of Droplets and Mixing in Multiphase Microfluidics at Low Values of the Reynolds and the Capillary Numbers

Joshua D. Tice, Helen Song, Adam D. Lyon, and Rustem F. Ismagilov*

Department of Chemistry, The University of Chicago, 5735 South Ellis Avenue, Chicago, Illinois 60637

Received March 4, 2003. In Final Form: June 11, 2003

This paper reports an experimental characterization of a simple method for rapid formation of droplets, or plugs, of multiple aqueous reagents without bringing reagents into contact prior to mixing. Droplet-based microfluidics offers a simple method of achieving rapid mixing and transport with no dispersion. In addition, this paper shows that organic dyes at high concentrations should not be used for the visualization of flow patterns and mixing of aqueous plugs in multiphase flows in this system (fluorinated carrier fluid and PDMS microchannels). It reports an inorganic dye that can be used instead. This work focuses on mixing in plugs moving through straight channels. It demonstrates that, when traveling through straight microchannels, mixing within plugs by steady recirculating flow is highly sensitive to the initial distribution of the aqueous reagents established by the eddy flow at the tip of the forming plug (twirling). The results also show how plugs with proper distribution of the aqueous reagents could be formed in order to achieve optimal mixing of the reagents in this system.

Introduction

This paper characterizes a method of using flow of immiscible fluids in microfluidic channels to form plugs containing multiple aqueous reagents, mix these reagents inside the plugs under optimal conditions in straight channels, and then reliably transport them through the channels. We define plugs as droplets that block the channel but do not wet the walls. This method solves two problems of microfluidics—mixing and dispersion. In the preliminary studies reported recently,[1] we have shown that droplet-based microfluidics can be successfully used to measure the rate of a chemical reaction on a millisecond time scale.

Dispersion of the solutes along the length of microfluidic channels is a problem associated with pressure-driven laminar flow; it is known as Taylor dispersion.[2] Dispersion leads to dilution of the samples injected into the microchannels, leads to cross-contamination of the samples, and limits the throughput of a microfluidic system. Some dispersion occurs due to flow—the pressure-driven flow profile is parabolic, with the fluid in the center of the capillary moving at a higher velocity than the fluid near the walls. Additional dispersion also occurs due to diffusion; even in the absence of flow, molecules are free to diffuse along the length of the channel. The dispersion due to flow can be removed by the use of electroosmotic flow (EOF), which has a flat flow profile,[3] although there is still some dispersion around bends of microchannels. EOF has been used very effectively for DNA separations.[4,5] However, EOF is not sufficiently robust for many applications: it requires high voltages, and it is highly sensitive to contaminations of the charged surfaces used to drive the flow. In addition, only low flow rates can be achieved using EOF.

The simplest solution to the dispersion problem is to localize the reagents within droplets surrounded by an immiscible fluid. Reagents no longer disperse along the whole length of the channel; rather dispersion is confined to the volume of the plug. A similar approach has been used for many years in biochemical blood analyzers,[6] although, in the case of analyzers, the stream of the aqueous reagent fluid wets the walls of the glass capillary and nonwetting air bubbles are used to segment the reagent fluid. The droplets have been successfully used to localize reagents in microfluidics.[4,7−11] An elegant droplet metering system has been used in a DNA analyzer.[4]

Mixing is the second problem associated with the laminar flow. Two streams injected into a channel at low Reynolds number[2], *Re*, flow laminar side-by-side, with mixing only by diffusion.[2,12,13] Rapid mixing of chemical reagents in microchannels is difficult to achieve, and a significant research effort has been devoted to solving this problem.[14−17] Hydrodynamic focusing,[18,19] injecting streams of reagents into a common channel as multiple lamina,[20] chaotic advection at intermediate[21] and low[16,17] values of *Re*, and the use of beads in microchannels[22] are some of the methods developed to enhance mixing. These methods do not eliminate dispersion, although chaotic advection has been shown to reduce it significantly.[16,17]

* Corresponding author.

(1) Song, H.; Tice, J. D.; Ismagilov, R. F. *Angew. Chem., Int. Ed.* **2002**, *42*, 768−772.
(2) Bird, R. B.; Stewart, W. E.; Lightfoot, E. N. *Transport Phenomena*; Wiley: New York, 2002.
(3) Medintz, I. L.; Paegel, B. M.; Blazej, R. G.; Emrich, C. A.; Berti, L.; Scherer, J. R.; Mathies, R. A. *Electrophoresis* **2001**, *22*, 3845−3856.
(4) Burns, M. A.; Johnson, B. N.; Brahmasandra, S. N.; Handique, K.; Webster, J. R.; Krishnan, M.; Sammarco, T.; Man, P. M.; Jones, D.; Heldsinger, D.; Mastrangelo, C. H.; Burke, D. T. *Science* **1998**, *282*, 484−487.
(5) Chou, H.-P.; Spence, C.; Scherer, A.; Quake, S. *Proc. Natl. Acad. Sci. U.S.A.* **1999**, *96*, 11−13.
(6) Snyder, L.; Levine, J.; Stoy, R.; Conetta, A. *Anal. Chem.* **1976**, *48*, 942.
(7) Burns, M. A. *Science* **2002**, *296*, 1818−1819.
(8) Fu, A. Y.; Spence, C.; Scherer, A.; Arnold, F. H.; Quake, S. R. *Nat. Biotechnol.* **1999**, *17*, 1109−1111.
(9) Cho, S. K.; Moon, H.; Fowler, J.; Kim, C. J. *Proc. ASME IMECE* **2001**, 1−7.
(10) Fowler, J.; Moon, H.; Kim, C. J. *Proc. 15th IEEE Conf. MEMS* **2002**, 97−100.
(11) Taniguchi, T.; Torii, T.; Higuchi, T. *Lab Chip* **2002**, *2*, 19−23.
(12) Kamholz, A. E.; Yager, P. *Sens. Actuator, B: Chem.* **2002**, *82*, 117−121.
(13) Ismagilov, R. F.; Stroock, A. D.; Kenis, P. J. A.; Whitesides, G.; Stone, H. A. *Appl. Phys. Lett.* **2000**, *76*, 2376−2378.

10.1021/la030090w CCC: $25.00
Published on Web 08/12/2003

All methods of mixing attempt to reduce the striation length, *stl* (m), the distance over which mixing can occur by diffusion. For diffusion in one dimension the mixing time, t_{mix} (s), is given by

$$t_{mix} = stl^2/2D \quad (1)$$

where D (m^2/s) is the diffusion constant. For a protein with a diffusion constant of $D = 10^{-10}$ m^2/s, reducing *stl* from 100 to 1 μm reduces t_{mix} from 50 s to 5 ms. A droplet moving through a channel develops recirculating flow, that enhances mixing by reducing the striation length.[23] Our preliminary results[1] indicated that mixing in moving plugs can be as fast as a few milliseconds. Thus, droplet-based microfluidics is attractive because it has the potential to solve both the mixing and dispersion problems.

This paper describes how we (i) experimentally characterized a simple method[1] for rapid formation of plugs of multiple reagents without bringing reagents into prior contact, (ii) designed a set of dyes useful for visualization of flow patterns inside aqueous plugs, (iii) determined that, in straight microchannels, mixing within plugs by the steady recirculating flow is highly sensitive to the initial distribution of the reagents, and (iv) established how plugs with proper distribution of the reagents can be formed in order to achieve rapid mixing in straight microchannels.

Experimental Section

Networks of microchannels with rectangular cross-sections were fabricated using rapid prototyping in poly(dimethylsiloxane) (PDMS).[24−26] The PDMS used was Dow Corning Sylgard Brand 184 Silicone Elastomer, and devices were sealed using a Plasma Prep II (SPI Supplies). The surfaces of the devices were rendered hydrophobic by baking the devices at 120 °C for 2−4 h.

In Figure 2, the red aqueous streams were McCormick red food coloring (water, propylene glycol, FD&C Reds 40 and 3, propylparaben), the green aqueous streams were McCormick green food coloring (water, propylene glycol, FD&C yellow 5, FD&C blue 1, propylparaben) diluted 1:1 with water, and the colorless streams were water. In all other figures, red aqueous streams were $Fe(SCN)_x^{(3-x)+}$ complexes prepared by mixing 0.067 M $Fe(NO_3)_3$ with 0.2 M KSCN. All remaining colorless aqueous streams were 0.2 M KNO_3. PFD used was a 10:1 mixture of perfluorodecalin (mixture of cis and trans, 95%, Acros Organics) and 1*H*,1*H*,2*H*,2*H*-perfluorooctanol (Acros Organics).

Aqueous solutions were pumped using 100 μL Hamilton Gastight syringes (1700 series, TLL) or 50 μL SGE gastight syringes. PFD was pumped using 1 mL Hamilton Gastight syringes (1700 series, TLL). The syringes were attached to microfluidic devices by means of Hamilton teflon needles (30 gauge, 1 hub). Syringe pumps from Harvard Apparatus (PHD 2000 Infusion pumps; specially ordered bronze bushings were attached to the driving mechanism to stabilize pumping) were used to infuse the aqueous solutions and PFD.

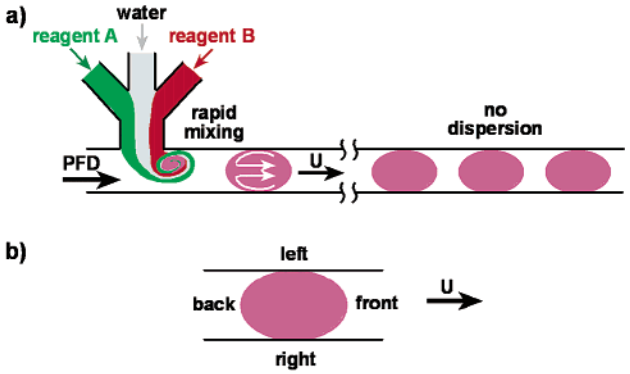

Figure 1. (a) Schematic illustration of the approach characterized in this paper to forming plugs of multiple aqueous solutions by injecting them into a stream of water-immiscible fluorinated fluid, PFD. Droplets were mixed rapidly by recirculation shown by white arrows. Plugs (droplets that block the channel but do not wet the walls) were transported with no dispersion. (b) Notation used throughout the paper to identify different regions of the plugs, relative to the direction of motion.

Microphotographs were taken with a Leica MZ12.5 stereomicroscope and a SPOT Insight Color digital camera (model #3.2.0, Diagnostic Instruments, Inc.). SPOT Advanced software (version 3.4.0 for Windows) was used to collect the images. Lighting was provided from a Machine Vision Strobe X-Strobe X1200 (20 Hz, 12 μF, 600 V, Perkin-Elmer Optoelectronics). To obtain an image, the shutter of the camera was opened for 1 s and the strobe light was flashed once with the duration of the flash being ~10 μs.

Images were analyzed using NIH Image software, Image J. Image J was used to measure periods and lengths of plugs from microphotographs such as those shown in Figure 7b. Periods corresponded to the distance from the center of one plug to the center of an adjacent plug, and the length of a plug was the distance from the extreme front to the extreme back of the plug (see Figure 1b for definitions of front and back).

Surface tensions were measured using the hanging drop method. A small (~1 μL) drop of the fluorinated fluid was extruded into ~1 mL of the aqueous solution inside a disposable optical cell. A microphotograph of the drop was taken with a CCD camera equipped with a zoom objective. The shape of the drop, determined by the balance of gravity and surface tension, was analyzed as described previously.[27−29]

To make measurements of the optical intensity of $Fe(SCN)_x^{(3-x)+}$ complexes in plugs, microphotographs were saved in CMYK color mode in Adobe Photoshop 6.0. Using the same program, the yellow color channels of the microphotographs were then isolated and converted to gray scale images, and the intensities of the gray scale images were inverted. The yellow color channel was chosen to reduce the intensity of bright reflections at the extremities of the plugs and at the interface between the plugs and the channel. Following the work done in Photoshop, regions of plugs containing high concentrations of $Fe(SCN)_x^{(3-x)+}$ complexes appeared white while regions of low concentration appeared black. Using Image J, the intensity was measured across a thin, rectangular region of the plug, located halfway between the front and back of the plug (white dashed lines in Figure 7a). The camera used to take the microphotographs of the system was not capable of making linear measurements of optical density. Therefore, our measurements of intensity were not quantitative. Several of the plots in

(14) Auroux, P.-A.; Iossifidis, D.; Reyes, D. R.; Manz, A. *Anal. Chem.* **2002**, *74*, 2623−2636.
(15) Auroux, P.-A.; Iossifidis, D.; Reyes, D. R.; Manz, A. *Anal. Chem.* **2002**, *74*, 2637−2652.
(16) Stroock, A. D.; Dertinger, S. K.; Whitesides, G. M.; Ajdari, A. *Anal. Chem.* **2002**, *74*, 5306−5312.
(17) Stroock, A. D.; Dertinger, S. K. W.; Ajdari, A.; Mezic, I.; Stone, H. A.; Whitesides, G. M. *Science* **2002**, *295*, 647−651.
(18) Knight, J. B.; Vishwanath, A.; Brody, J. P.; Austin, R. H. *Phys. Rev. Lett.* **1998**, *80*, 3863−3866.
(19) Pabit, S. A.; Hagen, S. J. *Biophys. J.* **2002**, *83*, 2872−2878.
(20) Bessoth, F. G.; deMello, A. J.; Manz, A. *Anal. Commun.* **1999**, *36*, 213-215.
(21) Liu, R. H.; Stremler, M. A.; Sharp, K. V.; Olsen, M. G.; Santiago, J. G.; Adrian, R. J.; Aref, H.; Beebe, D. J. *J. Microelectromech. Syst.* **2000**, *9*, 190−197.
(22) Seong, G. H.; Crooks, R. M. *J. Am. Chem. Soc.* **2002**, *124*, 13360−13361.
(23) Handique, K.; Burns, M. A. *J. Micromech. Microeng.* **2001**, *11*, 548−554.
(24) McDonald, J. C.; Whitesides, G. M. *Acc. Chem. Res.* **2002**, *35*, 491−499.
(25) McDonald, J. C.; Duffy, D. C.; Anderson, J. R.; Chiu, D. T.; Wu, H. K.; Schueller, O. J. A.; Whitesides, G. M. *Electrophoresis* **2000**, *21*, 27−40.
(26) Duffy, D. C.; McDonald, J. C.; Schueller, O. J. A.; Whitesides, G. M. *Anal. Chem.* **1998**, *70*, 4974−4984.
(27) Hansen, F. K. *J. Colloid Interface Sci.* **1993**, *160*, 209−217.
(28) Hansen, F. K.; Rodsrud, G. *J. Colloid Interface Sci.* **1991**, *141*, 1−9.
(29) Neumann, A. W.; Spelt, J. K. *Applied Surface Thermodynamics*; Marcel Dekker: New York, 1995.

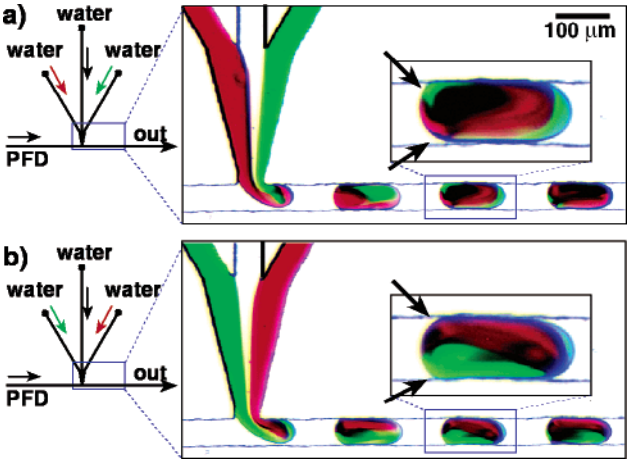

Figure 2. Concentrated solutions of organic dyes cannot be used to visualize true flow patterns and mixing inside plugs described in this paper because they perturbed the flow inside plugs. Left: Diagram of the microfluidic network. Right: Microphotographs of the plug-forming region of the microfluidic network. The colored aqueous streams were solutions of red and green food dyes. Plugs were traveling at 50 mm s^{-1}. The insets show enlarged microphotographs of plugs and their flow patterns. Arrows emphasize the difference in contact angles of the green and the red dyes with PDMS, indicating preferential wetting of the surface of the channels by the green dye.

the graphs of intensity versus relative position across the channel (Figure 7c) were shifted vertically by <50 units of intensity to adjust for nonuniform illumination of different parts of the images. These adjustments were justified because the shape of the distribution rather than absolute concentration was discussed in the paper.

Results and Discussion

Formation of a plug of multiple reagents[1] is schematically shown in Figure 1a. Two reagent streams were combined in a microchannel, separated by an inert stream. Since the flow was characterized by low values of the *Re*, the three streams remained laminar. The streams were continuously injected into a stream of flowing carrier fluid where they broke up into plugs transported by the carrier fluid. Microfluidic devices were fabricated using PDMS.[24−26] We chose perfluorodecaline (PFD) as the water immiscible carrier fluid because fluorinated fluids, in contrast to hydrocarbon fluids, do not swell PDMS.

Visualization. We visualized flow patterns inside moving plugs by injecting marked streams of fluid into a plug and monitored the distribution of the marker as the plug proceeded through the channel. Marking streams in microchannels with absorption dyes requires high concentration of the dye, because thin microchannels provide only a short optical path. All organic dyes that we investigated, including the food dyes shown in Figure 2, affected the interfacial properties of aqueous solutions when dissolved at high concentrations. Therefore, visualizations made with these dyes were not representative of the flow patterns in plugs composed of dilute aqueous solutions.

By comparing Figure 2a and b, it becomes apparent that our food dyes did not act as inert markers in the aqueous phase (Figure 2). If the dyes acted as inert markers, one would expect that switching the inlets through which the red and green streams enter the plug-forming region would lead to the formation of plugs with complementary flow patterns (flow patterns with switched colors but otherwise identical). This is not what was observed (Figure 2)—the gross features of the flow patterns, and

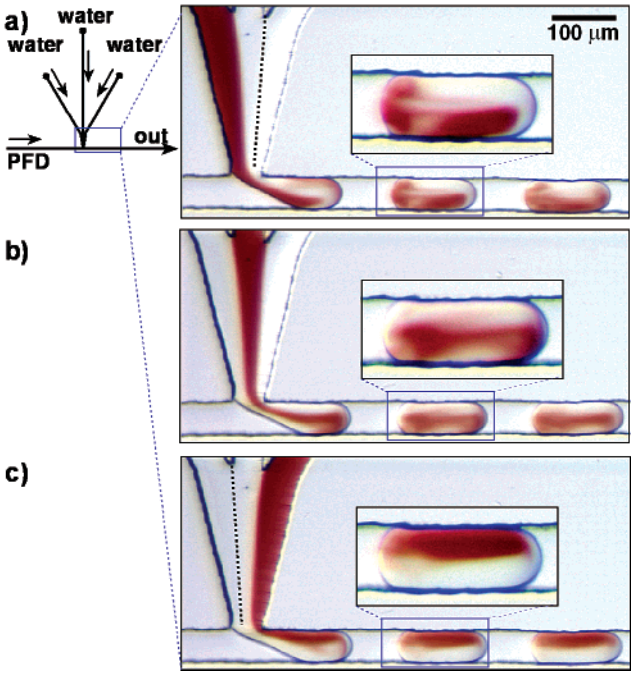

Figure 3. Aqueous solutions of $Fe(SCN)_x^{(3-x)+}$ complexes and KNO_3 can be used to visualize flow patterns and mixing in plugs. Left: Diagram of the microfluidic network. Right: Microphotographs of the plug-forming region of the microfluidic network. The insets show enlarged microphotographs of plugs and their flow patterns. Changing the position of the dyed stream yielded plugs with complementary (switched) colored regions that were characteristic of the same flow pattern—for example, white areas in part a correspond to red areas in either part b or c. Plugs were traveling at 50 mm s^{-1}.

not just their colors, changed when the two streams were switched. The shape of the plugs also changed (black arrows in Figure 2). We have not characterized the details of the flow of food dyes in microchannels—a better-defined system where both the viscosity and interfacial tension can be varied independently would be required for a conclusive study. Nevertheless, these data were sufficient to conclude that organic dyes at high concentrations were unsuitable for visualization of flow patterns in aqueous plugs of multiphase flow in this system.

To observe flow patterns without perturbing the flow in aqueous plugs, we used a red aqueous solution of an inorganic complex $Fe(SCN)_x^{(3-x)+}$ ($x \sim 3$, absorption maximum $\lambda_{max} \sim 480$ nm, extinction coefficient $\epsilon \sim 5 \times 10^3$ cm^{-1} M^{-1}) prepared by mixing 0.067 M $Fe(NO_3)_3$ with 0.2 M KSCN (the viscosity of the solution of the complex was 1.08 ± 0.05 mPa s). The two colorless aqueous streams were 0.2 M KNO_3 (viscosity 1.00 ± 0.05 mPa s). Both $Fe(SCN)_x^{(3-x)+}$ and KNO_3 solutions had interfacial tension with the fluorinated carrier fluid of 12−14 mN/m. These solutions did not perturb the flow patterns inside plugs (Figure 3). Switching the position of the colored stream leads to the formation of plugs with complementary distribution of the dye; for example, white areas in plugs shown in Figure 3a corresponded to dark areas in plugs shown in Figure 3b and c. Flow patterns within plugs were reproducible. At different flow rates, flow patterns were similar except for blurring by diffusion at lower flow rates, consistent with the low value of *Re* for these flows. We used these aqueous solutions in all subsequent experiments.

Formation of Plugs—Surface Tension and the Capillary Number. To obtain clean transport of the reagents, the carrier fluid must wet the walls of the

microchannels preferentially over the aqueous phase. If this condition is satisfied, the aqueous phase does not come in contact with the walls and remains separated from the walls by a thin layer of the carrier fluid;[30,31] the plugs are stable and do not leave any residue behind as they are transported through the channels. To achieve this condition,[29] the surface tension at the water/PDMS interface (~38 mN/m)[32] has to be higher than the surface tension at the water/PFD interface (~55 mN/m). We added 1*H*,1*H*,2*H*,2*H*-perfluorooctanol to PFD as a surfactant, which reduced the surface tension at the water/PFD interface. Using the hanging drop method,[27−29] we measured the surface tension at the interface of water (or various aqueous buffers or solutions of $Fe(SCN)_x^{(3-x)+}$ complexes) and the fluorinated 1*H*,1*H*,2*H*,2*H*-perfluorooctanol/PFD mixture to be 12−14 mN/m. In this paper we refer to this mixture of fluorinated fluids as carrier fluid or simply as PFD.

The surface tension at the water/PFD interface must be sufficiently high in order to avoid destruction of plugs by shear. Formation of plugs can be characterized by the dimensionless Capillary number, *Ca*,

$$Ca = U\mu/\gamma \qquad (2)$$

where U (m s^{-1}) is the velocity of the flow, γ (N m^{-1}) is the surface tension at the water/PFD interface, and μ (kg m^{-1} s^{-1}) is the viscosity of the fluid. U was determined by dividing the total volumetric flow rate by the cross-sectional area of the channel. The viscosity of PFD is 5.10 × 10^{-3} N m^{-1}, and the viscosity of water is 1.00 × 10^{-3} N m^{-1}. Water-in-oil droplets are commonly formed in microchannels.[33−35] When shear is used at high values of *Ca*, the diameter of the droplets r (m) is then described by the equation[33,36]

$$r \sim w\gamma/(\mu U) = w/Ca \qquad (3)$$

where w (m) is the cross-sectional dimension of the channel and U/w is the shear rate (s^{-1}). At values of $Ca > 1$, droplets with the diameter smaller than the dimensions of the channel form. Under these conditions, the size of droplets linearly depends on the inverse of the flow velocity (eq 3), and droplets of various sizes form a range of interesting patterns.[33]

We operated our system at low values of *Ca* (< ~0.1). Equation 3 did not predict the size of plugs in our system. The length of plugs was virtually independent of the total flow rate (Figure 4a and Figure 5) and of *Ca*. In addition, the period (p (m), the center-to-center distance between adjacent plugs) remained relatively constant as the flow rate (and *Ca*) was varied (Figure 4a). Assuming that the period is known, then the mass-conservation can be used to estimate the length of plugs l (m) from the "water fraction", *wf*—the value of $V_w/(V_w + V_f)$, where V_w and V_f are the relative volumetric flow rates of water, V_w (μL/min), and the fluorinated fluid, V_f (μL/min) (eq 4).

$$l = pV_w/(V_w + V_f) = p \times wf \qquad (4)$$

The length of plugs could be easily controlled by varying the relative volumetric flow rates of the aqueous and fluorous streams (Figure 4b). Short plugs formed when the flow rate of the aqueous stream was lower than that of the fluorous stream, and long plugs formed when the

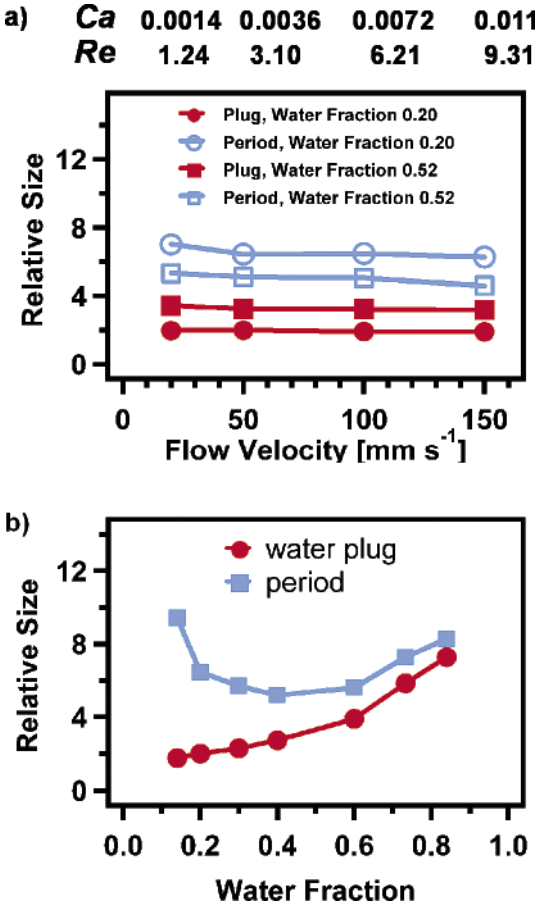

Figure 4. Data showing the spatial periods and the lengths of plugs as a function of (a) total flow velocity and (b) water fraction (defined in text). Values of Capillary (*Ca*) and Reynolds (*Re*) numbers are also shown. Plugs in part b are traveling at 50 mm s^{-1}. All measurements of length are reported relative to the width of channels (50 μm). Relative size is defined as the ratio of the length of the plug to the width of the channel.

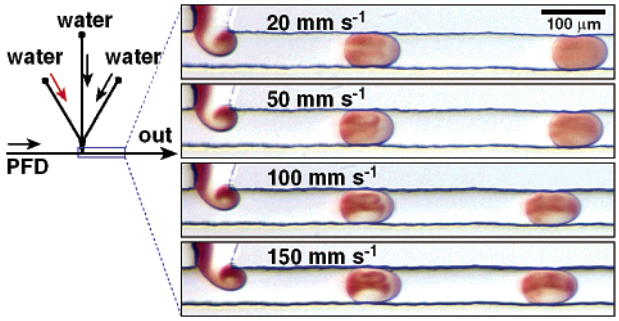

Figure 5. Microphotographs illustrating weak dependence of periods, length of plugs, and flow patterns inside plugs on total flow velocity. Left: Diagram of the microfluidic network. Right: Microphotographs of plugs formed at the same water fraction (0.20), but at different total flow velocities. The Capillary numbers were 0.0014, 0.0036, 0.0072, and 0.011, respectively, from top to bottom. The corresponding Reynolds numbers were 1.24, 3.10, 6.21, and 9.31.

(30) Bico, J.; Quere, D. *J. Fluid Mech.* **2002**, *467*, 101−127.
(31) Bico, J.; Quere, D. *J. Colloid Interface Sci.* **2002**, *247*, 162−166.
(32) Reiter, G.; Khanna, R.; Sharma, A. *Phys. Rev. Lett.* **2000**, *85*, 1432−1435.
(33) Thorsen, T.; Roberts, R. W.; Arnold, F. H.; Quake, S. R. *Phys. Rev. Lett.* **2001**, *86*, 4163−4166.
(34) Sugiura, S.; Nakajima, M.; Seki, M. *Langmuir* **2002**, *18*, 5708−5712.
(35) Anna, S. L.; Bontoux, N.; Stone, H. A. *Appl. Phys. Lett.* **2003**, *82*, 364−366.
(36) Taylor, G. I. *Proc. R. Soc. London A* **1934**, *146*, 501−523.

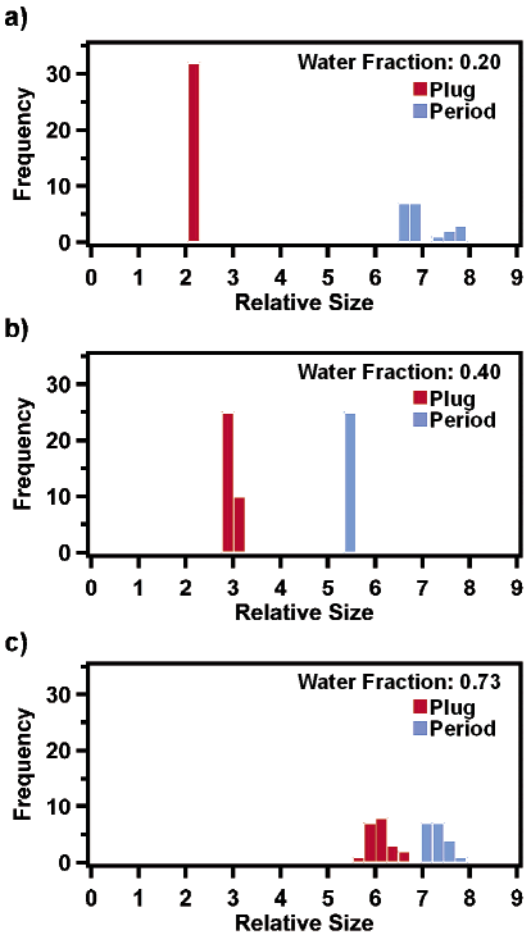

Figure 6. Histograms demonstrating the distribution of periods and lengths of plugs where the water fractions were (a) 0.20, (b) 0.40, and (c) 0.73. The total flow velocity was 50 mm s^{-1}, $Ca = 0.0036$, and $Re = 3.10$ in all cases. The period p (m) is the center-to-center distance between adjacent plugs. "Frequency" refers to the number of plugs or periods of a particular size in the histogram.

flow rate of the aqueous stream was higher than that of the fluorous stream. The dependence of the length of the plugs on the water fraction deviates from the linearity suggested by eq 4 for two reasons: (i) This equation is approximate because it ignores the curvature at the sides of the plugs and assumes that plugs are parallelepipeds. This assumption predicts length that is too low for the small, almost spherical plugs. (ii) The period p itself depends on the water fraction. The period should become infinite at extreme values of $wf = 0$ and $wf = 1$. As water fraction was changed from ~0.15 to ~0.85, the period varied by a factor of ~2, passing through a minimum at the water fraction of ~0.50 (Figure 4b). This dependence of p introduced additional positive curvature to the graph of l versus wf in Figure 4b. Despite these deviations, the length of plugs l could be easily estimated.

Plugs of constant length could be formed reproducibly at intermediate values of water fraction, $0.20 < wf < 0.80$ (Figure 6). We have collected statistics describing the lengths of plugs l formed when water fraction was set to 0.20, 0.40, and 0.73. Irregular motion of the syringe pumps induced fluctuations in relative flow rates; therefore, fluctuations in period were observed (for these experiments, we used two separate syringe pumps for the fluorous and aqueous phases). The fluctuations of flow rates affected the water fraction and became especially noticeable when the flow rates of the aqueous and the fluorous streams became significantly different (Figure 6a and c). The period was also more sensitive to changes in water fraction at extreme values of water fraction (Figure 4b). The length of plugs formed in flows driven by a syringe pump varied by about 3−20% of their length, depending on the water fraction. This level of monodispersity was adequate for the studies of mixing described below.

Mixing. Mixing in moving plugs occurs by recirculating flow (white arrows in Figure 1) caused by the shearing interactions of the fluid inside the plug with the stationary wall.[37] These closed recirculation flows are localized in the left and right halves of the plug (Figure 1). Theoretical studies by Burns[23] indicate that, for ideal initial conditions, the recirculating flow reduces the striation length, *stl* (m):

$$stl(d) = stl(0) \times l/d \qquad (5)$$

as a function of l/d, where d (m) is the distance traveled by the plug and l (m) is the length of the plug;[23] $stl(0)$ is the initial striation length in a plug, and $stl(d)$ is the striation length after a plug has traveled a distance d through the channel.

According to eq 5, reduction of *stl* by these steady flows depends on both d and l. One complete cycle of recirculation occurs when the plug has traveled its length, $d = l$. After d/l complete cycles of recirculation, the *stl* will have decreased inversely proportionately to the number of cycles. Therefore, eq 5 predicts that shorter plugs will mix in a shorter distance, d, and therefore in a shorter time, t_{mix}, at constant U. This prediction is certainly valid under ideal initial conditions.[23] In our system, the process of plug formation leads to a nonideal distribution of the solutions in the plug, and mixing may occur faster or much slower than predicted for the ideal initial conditions.

When the two solutions to be mixed are initially located in the front and back halves (defined in Figure 1b) of the plug, then recirculation effectively reduces the *stl* and this results in efficient mixing after several d/l cycles (Figure 7a1). However, if the two solutions are localized in the left and right halves (defined in Figure 1b) of the plug, then the *stl* is not affected by recirculating flows and therefore mixing is inefficient (Figure 7a2).

The initial distribution of the marker in the plug depended strongly on the details of plug formation. As the stationary aqueous plug was extruded into the flowing carrier fluid, shearing interactions between the flow of the carrier fluid and the aqueous phase induced an eddy that redistributed the solution of the marker to different regions of the plug. We refer to the formation of this eddy as "twirling". Inertial effects did not induce twirling; twirling was present at both the low values of *Re* and the high values of *Re*, and it occurred at all flow velocities, although the flow pattern of this eddy was slightly affected by the velocity (Figure 5).

Twirling redistributed the marker by transferring it from the right to the left side of the plug (Figure 7b). Twirling was present during the formation of plugs of all lengths, but its importance for mixing depended on the length of the plug. Twirling occurred only at the tip of the forming plug before the tip made contact with the right (defined in Figure 1b) wall of the microchannel. The amount of twirling in a plug was related to the amount of the carrier fluid that flowed past the tip; this amount was significantly larger for short plugs than for long plugs

(37) This interaction may be modulated by the thin wetting layer of the carrier fluid separating the droplet from the wall, but this effect is small because the carrier fluid has slightly higher viscosity than the aqueous fluids.

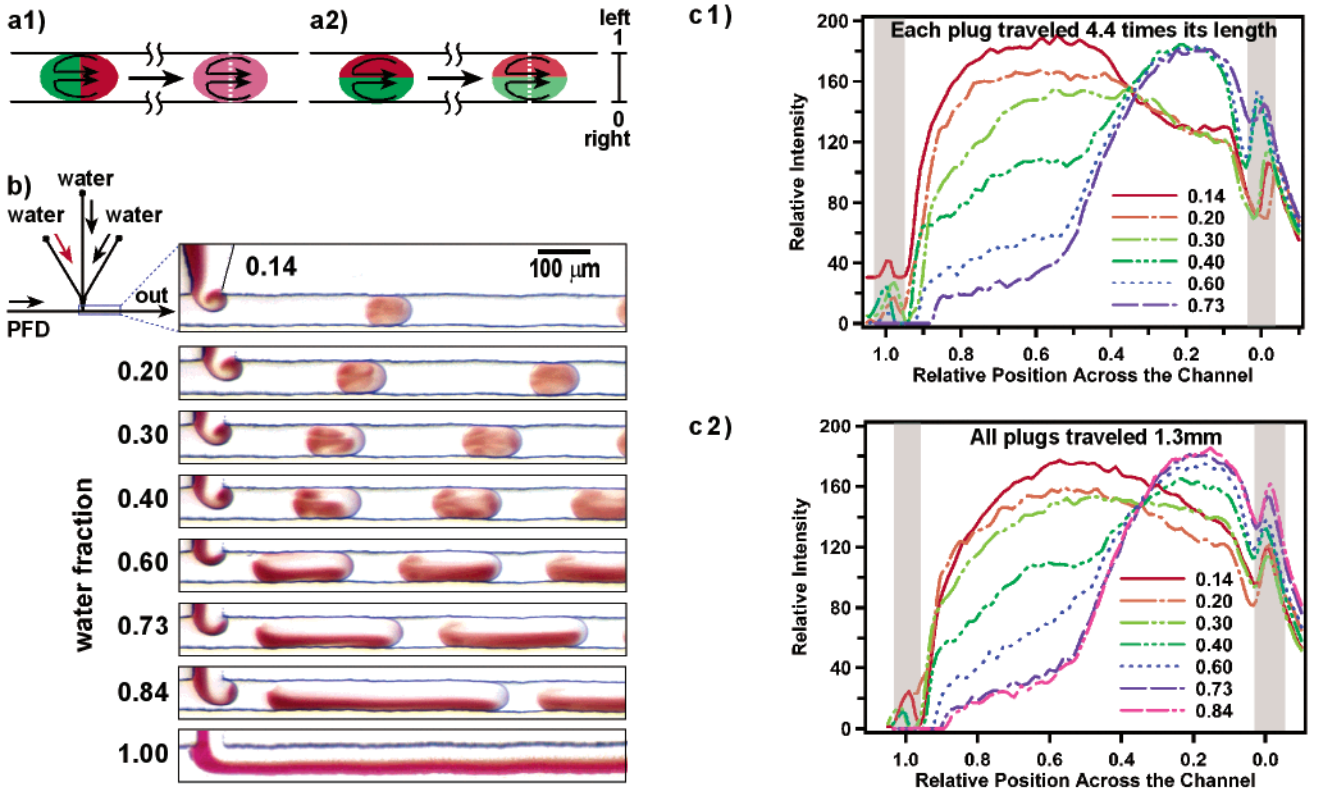

Figure 7. Effects of initial conditions on mixing by recirculating flow inside plugs moving through straight microchannels. (a1) Recirculating flow (shown by black arrows) efficiently mixed solutions of reagents that were initially localized in the front and back halves of the plug. Notations of front, back, left, and right are the same as those in Figure 1b. (a2) Recirculating flow (shown by black arrows) did not efficiently mix solutions of reagents that were initially localized in the left and right halves of the plug. (b) Left: Schematic diagram of the microfluidic network. Right: Microphotographs of different length plugs near the plug-forming region of the microfluidic network, for water fractions of 0.14−1.00. Plugs were traveling at 50 mm s^{-1}. (c1) A graph showing the relative optical intensity of $Fe(SCN)_x^{(3-x)+}$ complexes in plugs of different lengths. Intensities were measured from left ($x = 1.0$) to right ($x = 0.0$) across the width of a plug (shown by white dashed lines in parts a1 and a2) after the plug had traveled 4.4 times its length through the straight microchannel. The gray shaded areas indicate the walls of the microchannel. (c2) Same as part c1, except each plug had traveled 1.3 mm. The d/l for each water fraction was 15.2 ($wf = 0.14$), 13.3 ($wf = 0.20$), 11.7 ($wf = 0.30$), 9.7 ($wf = 0.40$), 6.8 ($wf = 0.60$), 4.6 ($wf = 0.73$), and 2.7 ($wf = 0.84$).

(Figure 7b). Twirling affected only a small fraction of the long plugs and had a small effect on the distribution of the marker in these plugs (Figure 7b). Recirculating flow did not significantly accelerate mixing in longer plugs (Figure 7b, $wf = 0.73$) because not enough of the marker was transferred into the left side of the plug—the initial conditions for mixing in large plugs were similar to those shown in Figure 7a2. Mixing in the longest plugs was similar to mixing in a laminar flow in the absence of PFD (Figure 7b, $wf = 1.00$). In contrast, twirling accelerated mixing for shorter plugs (Figure 7b, $wf = 0.30$). Here, twirling redistributed the marker just enough into the left side such that nearly ideal initial conditions were created, like those in Figure 7a1. Under these conditions, we observed that the initial striation length was reduced by the formation of a spiral flow pattern shown schematically in Figure 1a. However, for even shorter plugs, mixing was worse (Figure 7b, $wf = 0.14$ and $wf = 0.20$) due to "overtwirling". In this case, too much of the marker was transferred into the left side of the plug. When overtwirling occurred, mixing was less efficient because initial conditions resembled those observed for longer plugs (Figure 7b, $wf = 0.40$), except that the red markers occupied the opposite side of the plug.

We have created two intensity plots (Figure 7c) that show the relative concentration of the marker within the plug across the channel at the different water fractions (Figure 7b). For these plots, the general shape of each curve can qualitatively identify which initial condition results in the most efficient mixing. The most efficient mixing corresponds to a curve with minimal fluctuations in intensity (the marker is evenly distributed across the plug). To further investigate the effects of twirling on mixing, intensity was measured across each plug after it traveled a distance d of 4.4 times its length l (Figure 7c1). If twirling is ignored, under these conditions of constant d/l for all plugs, eq 5 predicts equivalent mixing in all plugs. Equation 5 is undoubtedly valid[23] for the ideal initial conditions (Figure 7a1), and deviations from the predictions of the equation can be safely attributed to the effect of twirling. For the longer plug with $wf = 0.73$ and $wf = 0.60$, the plugs were not well mixed: the relative intensity curve was much higher on the right side of the plug than on the left side of the plug. For the shorter plug with $wf = 0.30$, the mixing curve was fairly smooth and so the plug was well mixed. For $wf = 0.30$, we estimated mixing time ~ 25 ms under these conditions. Mixing time could be reduced further by increasing the flow rate, but we have not been able to reach the ~2 ms mixing time observed for mixing by chaotic advection.[1] This fact is consistent with the lower mixing efficiency of steady recirculating flows rather than that of time-dependent flows.[38] For the shortest plugs with $wf = 0.14$, the relative intensity was higher on the left side of the plug, and

(38) Ottino, J. M. *The Kinematics of Mixing: Stretching, Chaos, and Transport*; Cambridge University Press: Cambridge, 1989.

therefore, this plug was overtwirled, in agreement with the images in Figure 7b.

The second graph (Figure 7c2) shows the intensity measured across each plug after it traveled a fixed distance, $d = 1.3$ mm. Except for the longest plug of $wf = 0.73$, all plugs have traveled a longer distance in the second graph than in the first graph. Therefore, in this second graph, more mixing took place and the intensity curves showed more uniform distribution of the marker, especially for short plugs. For the longer plugs, the intensity curves remained similar to those observed in Figure 7c1. Under these conditions, if twirling was ignored, one would have expected that the shortest plugs ($wf = 0.14$) with the highest d/l ratio would have mixed faster than medium plugs ($wf = 0.30$). However, this was not the case, and we still saw the effects of overtwirling. We concluded that twirling was the most important factor in determining ideal conditions for mixing in plugs moving through straight microchannels.

Conclusions

In this paper, we have characterized experimentally a simple method for rapid formation of plugs of multiple reagents without bringing the reagents into prior contact. Plugs were formed at low values of the Capillary number and at low values of the Reynolds number, and therefore, the length of plugs and the flow patterns within them were only weakly dependent on the flow velocity. In addition, we have shown that organic dyes at high concentrations should not be used for the visualization of flow patterns and mixing in these systems. We found that an inorganic complex with a high extinction coefficient may be used to visualize unperturbed flow patterns in multiphase fluid flow. We used these experimental results to establish that, in straight microfluidic channels, mixing by steady recirculating flow within plugs was sensitive to the initial distribution of the reagents, and we described how the process of formation of the plugs affected this initial distribution. To achieve optimal mixing of the reagents in straight microchannels, plugs with the proper initial distribution of the reagents could be formed simply by adjusting the relative flow rates of the aqueous and fluorous streams to the experimentally determined optimal value. The following questions remain to be answered: What are the factors that determine the period of the instability leading to the formation of plugs? Is mixing by chaotic advection in plugs[1] less dependent on the initial conditions and the length of plugs than the mixing by twirling described here? What is the range of viscosities and interfacial tensions of the solutions and the carrier fluids where these two methods of mixing are applicable? These questions will serve as the basis for future experimental and theoretical work and will complement current developments in multiphase microfluidics.[39−42] We are beginning to use these systems as the basis of a microfluidic platform with rapid mixing and transport with no dispersion, useful for controlling chemical and biochemical systems on time scales from milliseconds to days. We are developing this platform for applications in rapid chemical synthesis and biochemical analysis, especially in proteomics.[43−46]

Acknowledgment. This work was supported by the Camille and Henry Dreyfus New Faculty Award, the Research Innovation Award from Research Corporation, by Chicago MRSEC funded by NSF, and by the Predoctoral Training Grant (H.S.) of the NIH (GM 08720). This work has been performed at the Chicago MRSEC microfluidics facility. Photolithography was performed at MAL of UIC. We thank Professors Sidney R. Nagel and Thomas A. Witten for helpful discussions on the subjects of the Capillary number and the mechanisms of eddy formation.

LA030090W

(39) Ajmera, S. K.; Delattre, C.; Schmidt, M. A.; Jensen, K. F. *Sens. Actuator, B: Chem.* **2002**, *82*, 297−306.
(40) Losey, M. W.; Schmidt, M. A.; Jensen, K. F. *Ind. Eng. Chem. Res.* **2001**, *40*, 2555−2562.
(41) Zhao, B.; Viernes, N. O. L.; Moore, J. S.; Beebe, D. J. *J. Am. Chem. Soc.* **2002**, *124*, 5284−5285.
(42) Zhao, B.; Moore, J. S.; Beebe, D. J. *Science* **2001**, *291*, 1023−1026.
(43) Fields, S. *Science* **2001**, *291*, 1221.
(44) Ideker, T.; Thorsson, V.; Ranish, J. A.; Christmas, R.; Buhler, J.; Eng, J. K.; Bumgarner, R.; Goodlett, D. R.; Aebersold, R.; Hood, L. *Science* **2001**, *292*, 929−934.
(45) Lee, K. H. *Trends Biotechnol.* **2001**, *19*, 217−222.
(46) Zhou, Z. L.; Licklider, L. J.; Gygi, S. P.; Reed, R. *Nature* **2002**, *419*, 182−185.